DOI: 10.1002/anie.200602866

Magnetic Nanoparticles

Magnetic Nanoparticles: Synthesis, Protection, Functionalization, and Application

*An-Hui Lu, E. L. Salabas, and Ferdi Schüth**

Keywords:
magnetic properties · nanoparticles · synthetic methods

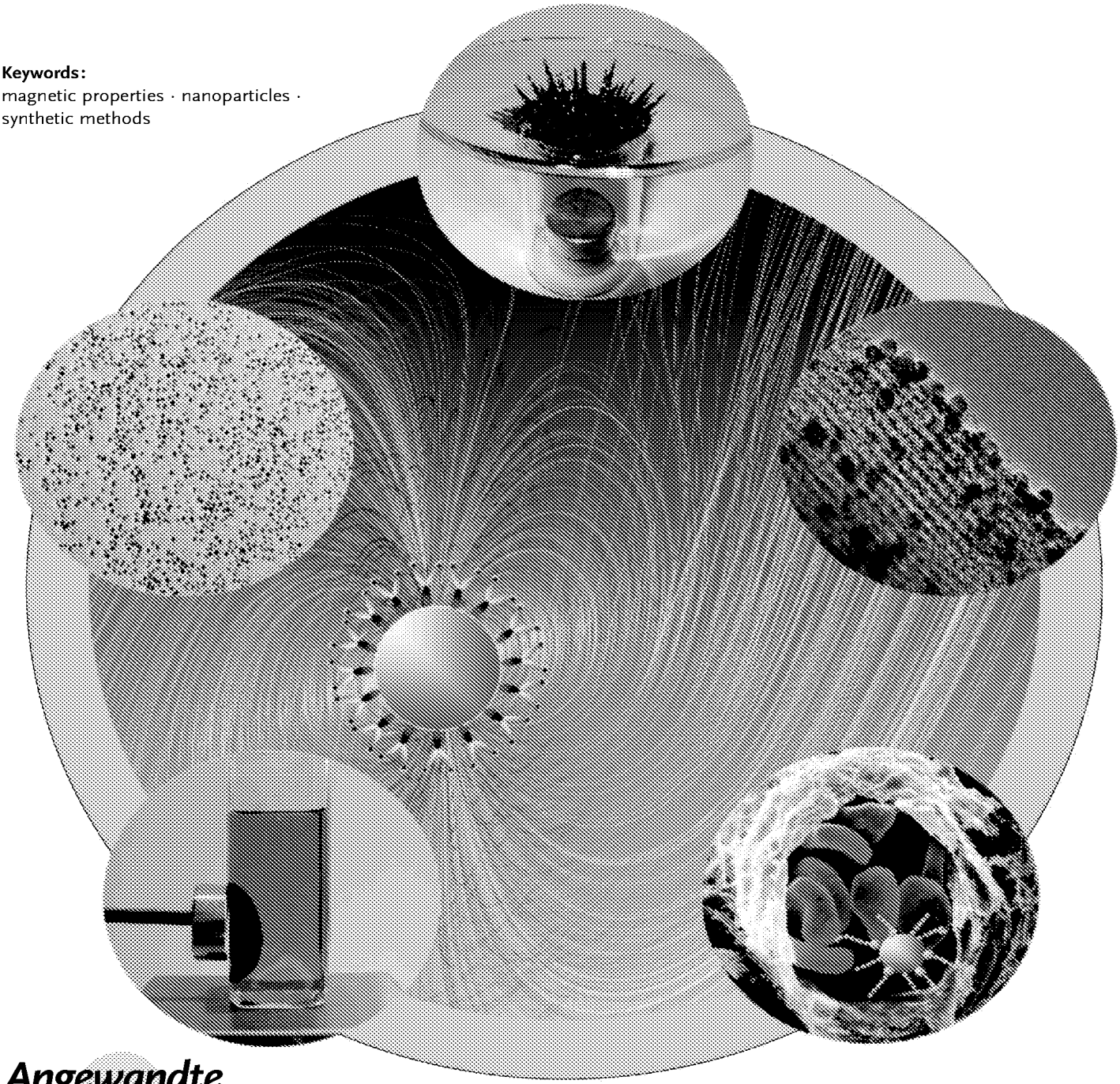

This review focuses on the synthesis, protection, functionalization, and application of magnetic nanoparticles, as well as the magnetic properties of nanostructured systems. Substantial progress in the size and shape control of magnetic nanoparticles has been made by developing methods such as co-precipitation, thermal decomposition and/or reduction, micelle synthesis, and hydrothermal synthesis. A major challenge still is protection against corrosion, and therefore suitable protection strategies will be emphasized, for example, surfactant/polymer coating, silica coating and carbon coating of magnetic nanoparticles or embedding them in a matrix/support. Properly protected magnetic nanoparticles can be used as building blocks for the fabrication of various functional systems, and their application in catalysis and biotechnology will be briefly reviewed. Finally, some future trends and perspectives in these research areas will be outlined.

From the Contents

1. Introduction

Magnetic nanoparticles are of great interest for researchers from a wide range of disciplines, including magnetic fluids,[1] catalysis,[2,3] biotechnology/biomedicine,[4] magnetic resonance imaging,[5,6] data storage,[7] and environmental remediation.[8,9] While a number of suitable methods have been developed for the synthesis of magnetic nanoparticles of various different compositions, successful application of such magnetic nanoparticles in the areas listed above is highly dependent on the stability of the particles under a range of different conditions. In most of the envisaged applications, the particles perform best when the size of the nanoparticles is below a critical value, which is dependent on the material but is typically around 10–20 nm. Then each nanoparticle becomes a single magnetic domain and shows superparamagnetic behavior when the temperature is above the so-called blocking temperature. Such individual nanoparticles have a large constant magnetic moment and behave like a giant paramagnetic atom with a fast response to applied magnetic fields with negligible remanence (residual magnetism) and coercivity (the field required to bring the magnetization to zero). These features make superparamagnetic nanoparticles very attractive for a broad range of biomedical applications because the risk of forming agglomerates is negligible at room temperature.

However, an unavoidable problem associated with particles in this size range is their intrinsic instability over longer periods of time. Such small particles tend to form agglomerates to reduce the energy associated with the high surface area to volume ratio of the nanosized particles. Moreover, naked metallic nanoparticles are chemically highly active, and are easily oxidized in air, resulting generally in loss of magnetism and dispersibility. For many applications it is thus crucial to develop protection strategies to chemically stabilize the naked magnetic nanoparticles against degradation during or after the synthesis. These strategies comprise grafting of or coating with organic species, including surfactants or polymers, or coating with an inorganic layer, such as silica or carbon. It is noteworthy that in many cases the protecting shells not only stabilize the nanoparticles, but can also be used for further functionalization, for instance with other nanoparticles or various ligands, depending on the desired application.

Functionalized nanoparticles are very promising for applications in catalysis, biolabeling, and bioseparation. Especially in liquid-phase catalytic reactions, such small and magnetically separable particles may be useful as quasi-homogeneous systems that combine the advantages of high dispersion, high reactivity, and easy separation. In the following, after briefly addressing the magnetic phenomena specific for nanoparticles, we focus mainly on recent developments in the synthesis of magnetic nanoparticles, and various strategies for the protection of the particles against oxidation and acid erosion. Further functionalization and application of such magnetic nanoparticles in catalysis and bioseparation will be discussed in brief. Readers who are interested in a more detailed treatment of the physical properties and behavior of these magnetic nanoparticles, or biomedical and biotechnology applications, are referred to specific reviews.[10–18]

2. Special Features of Magnetic Nanoparticles

Two key issues dominate the magnetic properties of nanoparticles: finite-size effects and surface effects which give rise to various special features, as summarized in

[*] Dr. A.-H. Lu, Dr. E. L. Salabas, Prof. Dr. F. Schüth
Max-Planck-Institut für Kohlenforschung
45470 Mülheim an der Ruhr (Germany)
Fax: (+49) 208-306-2395
E-mail: schueth@mpi-muelheim.mpg.de

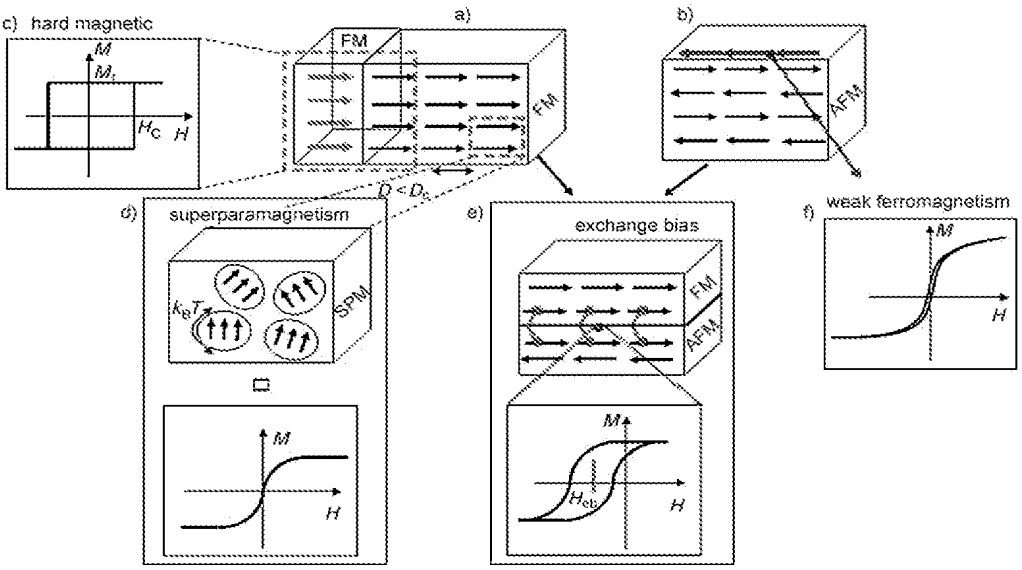

Figure 1. The different magnetic effects occurring in magnetic nanoparticles. The spin arrangement in a) a ferromagnet (FM) and b) an antiferromagnet (AFM); D = diameter, D_c = critical diameter. c) A combination of two different ferromagnetic phases (magenta arrows and black arrows in (a)) may be used for the creation of novel functional nanomaterials, for example, permanent magnets, which are materials with high remanence magnetization (M_r) and high coercivity (H_C), as shown schematically in the magnetization curve (c), d) An illustration of the magnetic moments in a superparamagnet (SPM). A superparamagnet is defined as an assembly of giant magnetic moments which are not interacting, and which can fluctuate when the thermal energy, $k_B T$, is larger than the anisotropy energy. Superparamagnetic particles exhibit no remanence or coercivity, that is, there is no hysteresis in the magnetization curve (d). e) The interaction (exchange coupling; linked red dots) at the interface between a ferromagnet and an antiferromagnet produces the exchange bias effect. In an exchange-biased system, the hysteresis is shifted along the field axis (exchange bias field (H_{eb}))and the coercivity increases substantially. f) Pure antiferromagnetic nanoparticles could exhibit superparamagnetic relaxation as well as a net magnetization arising from uncompensated surface spins (blue arrows in (b)). This Figure, is a rather simplistic view of some phenomena present in small magnetic particles. In reality, a competition between the various effects will establish the overall magnetic behavior.

Figure 1. Finite-size effects result, for example, from the quantum confinement of the electrons, whereas typical surface effects are related to the symmetry breaking of the crystal structure at the boundary of each particle. Without attempting to be exhaustive, these two issues will be addressed in Section 2.1 and 2.2. More complete reviews on magnetism in nanoscale systems can be found elsewhere.[19,20] Because there is no general agreement on the size limits for nanoparticles, in the following we use this term for particles with diameters ranging from 1 to 100 nm.

2.1. Finite-Size Effects

The two most studied finite-size effects in nanoparticles are the single-domain limit and the superparamagnetic limit. These two limits will be briefly discussed herein. In large magnetic particles, it is well known that there is a multi-domain structure, where regions of uniform magnetization are separated by domain walls. The formation of the domain walls is a process driven by the balance between the magnetostatic energy (ΔE_{MS}), which increases proportionally to the volume of the materials and the domain-wall energy (E_{dw}), which increases proportionally to the interfacial area between domains. If the sample size is reduced, there is a critical volume below which it costs more energy to create a domain wall than to support the external magnetostatic energy (stray field) of the single-domain state. This critical diameter typically lies in the range of a few tens of nanometers and depends on the material. It is influenced by the contribution from various anisotropy energy terms.

The critical diameter of a spherical particle, D_c, below which it exists in a single-domain state is reached when $\Delta E_{MS} = E_{dw}$, which implies $D_c \approx 18\frac{\sqrt{A K_{eff}}}{\mu_0 M^2}$, where A is the

An-Hui Lu received his B.S. in Chemical Engineering from Taiyuan University of Technology (China) in 1996 and his Ph.D. from the Institute of Coal Chemistry, Chinese Academy of Sciences in 2001. After postdoctoral work (as a Max-Planck research fellow and Alexander von Humboldt fellow) in the group of Prof. F. Schüth at the Max-Planck-Institut für Kohlenforschung, he was promoted to group leader in 2005. His research interests include synthesis and functionalization of nanostructured materials and magnetically separable catalysts, and their use in heterogeneous catalytic reactions.

Elena Lorena Salabas (née Bîzdoacă) received her B.S. (1996) and M.S. (2000) degrees in physics from the University of Bucharest, Romania. She obtained her Ph.D. in Physics from the University Duisburg-Essen, Germany in 2004. She was awarded the Lev Falicov Student Award (Denver-Colorado, 2002) of the American Vacuum Society for the Best Student Paper Award in the Magnetic Interfaces and Nanostructure Division. Currently she has a postdoctoral fellowship in the group of Prof. F. Schüth at the Max-Planck-Institut für Kohlenforschung, Mülheim. Her research focuses on the magnetism of nanostructured materials and exchange-biased systems.

exchange constant, K_{eff} is anisotropy constant, μ_0 is the vacuum permeability, and M is the saturation magnetization. Typical values of D_c for some important magnetic materials are listed in Table 1.[19]

Table 1: Estimated single-domain size for different spherical particles.

Material	D_c [nm]
hcp Co	15
fcc Co	7
Fe	15
Ni	55
$SmCo_5$	750
Fe_3O_4	128

A single-domain particle is uniformly magnetized with all the spins aligned in the same direction. The magnetization will be reversed by spin rotation since there are no domain walls to move. This is the reason for the very high coercivity observed in small nanoparticles.[21] Another source for the high coercivity in a system of small particles is the shape anisotropy.

The departure from sphericity for single-domain particles is significant and has an influence on the coercivity as is shown, for instance, in Table 2 for Fe nanoparticles.[20]

Table 2: The influence of the shape of Fe particles on the coercivity.

Aspect ratio (c/a)	H_C [Oe]
1.1	820
1.5	3300
2.0	5200
5.0	9000
10	10100

It must be remembered that the estimation of the critical diameter holds only for spherical and non-interacting particles. Particles with large shape anisotropy lead to larger critical diameters.

The second important phenomenon which takes place in nanoscale magnetic particles is the superparamagnetic limit. The superparamagnetism can be understood by considering the behavior of a well-isolated single-domain particle. The magnetic anisotropy energy per particle which is responsible for holding the magnetic moments along a certain direction can be expressed as follows: $E(\theta) = K_{eff} V \sin^2\theta$, where V is the particle volume, K_{eff} anisotropy constant and θ is the angle between the magnetization and the easy axis.

The energy barrier $K_{eff}V$ separates the two energetically equivalent easy directions of magnetization. With decreasing particle size, the thermal energy, $k_B T$, exceeds the energy barrier $K_{eff}V$ and the magnetization is easily flipped. For $k_B T > K_{eff} V$ the system behaves like a paramagnet, instead of atomic magnetic moments, there is now a giant (super) moment inside each particle (Figure 1d). This system is named a superparamagnet. Such a system has no hysteresis and the data of different temperatures superimpose onto a universal curve of M versus H/T.

The relaxation time of the moment of a particle, τ, is given by the Néel-Brown expression [Eq. (1)rsqb;[20] where k_B is the Boltzmann's constant, and $\tau_0 \approx 10^{-9}$ s.

$$\tau = \tau_0 \exp\left(\frac{K_{eff} V}{k_B T}\right) \quad (1)$$

If the particle magnetic moment reverses at times shorter than the experimental time scales, the system is in a superparamagnetic state, if not, it is in the so-called blocked state. The temperature, which separates these two regimes, the so-called blocking temperature, T_B, can be calculated by considering the time window of the measurement. For example, the experimental measuring time with a magnetometer (roughly 100 s) gives: $T_B = \frac{K_{eff} V}{30 k_B}$.

The blocking temperature depends on the effective anisotropy constant, the size of the particles, the applied magnetic field, and the experimental measuring time.

For example, if the blocking temperature is determined using a technique with a shorter time window, such as ferromagnetic resonance which has a $\tau \approx 10^{-9}$ s, a larger value of T_B is obtained than the value obtained from dc magnetization measurements. Moreover, a factor of two in particle diameter can change the reversal time from 100 years to 100 nanoseconds. While in the first case the magnetism of the particles is stable, in the latter case the assembly of the particles has no remanence and is superparamagnetic.

Many techniques are available to measure the magnetic properties of an assembly of magnetic nanoparticles. In the following, only some of the more important techniques are briefly discussed, and for more detailed information, the reader is referred to the cited references. SQUID magnetometry[22] and vibrating sample magnetometry (VSM)[23] are powerful tools to measure the sample's net magnetization. Like most conventional magnetization probes, both techniques are not element specific but rather measure the whole magnetization. Ferromagnetic resonance (FMR) probes the magnetic properties in the ground state and provides information about magnetic anisotropy, magnetic moment, relaxation mechanism of magnetization, and g-factor.[24] X-ray absorption magnetic circular dichroism (XMCD) is the method of choice to determine the orbital and spin magnetic moments. It is based on the changes in the absorption cross

Prof. Dr. Ferdi Schüth studied Chemistry and Law at the Westfälische-Wilhelms-Universität in Münster/Germany, where he received the Ph.D. in Chemistry in 1988 and the State Examination in Law in 1989. 1988/89 he was a post-doc in the group of L. D. Schmidt at the Department of Chemical Engineering at the University of Minnesota. 1989–1995 he worked on his Habilitation with K. Unger in Mainz and for five months in 1993 with G. Stucky at Santa Barbara. In 1995 he became full professor at the Johann-Wolfgang-Goethe Universität Frankfurt. In 1998 he was appointed Director at the Max-Planck-Institut für Kohlenforschung, Mülheim. He serves on the editorial board of several international journals and is also cofounder of hte AG in Heidelberg.

section of a magnetic material and uses circularly polarized photons.[25,26] The magneto-optical Kerr effect (MOKE) is also used as a magnetization-measuring tool.[25] The basic principle behind MOKE is that as polarized light interacts with a magnetic material the polarization of the light can change. In principle, this method is very useful for qualitative magnetic characterization, for imaging domain patterns, and for measuring the magnetic hysteresis. Qualitative information on magnetization, exchange and anisotropy constants from magnon spectra are provided by Brillouin light scattering (BLS).[27] This technique is an optical method capable of detecting and determining the frequency of magnetic excitations (surface spin waves) that can interact with visible photons in magnetic systems.

A simple and rapid way to estimate the blocking temperature is provided by dc magnetometry measurements, in which a zero-field-cooled/field-cooled procedure is employed. Briefly, the sample is cooled from room temperature in zero magnetic field (ZFC) and in a magnetic field (FC). Then a small magnetic field is applied (about 100 Oe) and the magnetization is recorded on warming. As temperature increases, the thermal energy disturbs the system and more moments acquire the energy to be aligned with the external field direction. The number of unblocked, aligned moments reaches a maximum at T_B. Above the blocking temperature the thermal energy is strong enough to randomize the magnetic moments leading to a decrease in magnetization.

A distribution of the particle sizes results in a distribution of the blocking temperatures. As pointed out already, the above discussion about the time evolution of the magnetization only holds for particles with one single-domain. Taking into account the magnetic interactions between nanoparticles which have a strong influence on the superparamagnetic relaxation, the behavior of the system becomes more complicated. The main types of magnetic interactions which can be present in a system of small particles are: a) dipole–dipole interactions, b) direct exchange interactions for touching particles, c) superexchange interactions for metal particles in an insulating matrix, d) RKKY (Ruderman-Kittel-Kasuya-Yosdida) interactions for metallic particles embedded in a metallic matrix.[19] Dipolar interactions are almost always present in a magnetic particle system and are typically the most relevant interactions. They are of long-range character and are anisotropic. From an experimental point of view, the problem of interparticle interactions is very complex. First, it is very complicated to separate the effects of interactions from the effects caused by the random distributions of sizes, shapes, and anisotropy axes. Second, several interactions can be present simultaneously in one sample. This situation makes it even more complicated to assign the observed properties to specific interactions.

2.2. Surface Effects

As the particles size decreases, a large percentage of all the atoms in a nanoparticle are surface atoms, which implies that surface and interface effects become more important. For example, for face-centered cubic (fcc) cobalt with a diameter of around 1.6 nm, about 60% of the total number of spins are surface spins.[19] Owing to this large surface atoms/bulk atoms ratio, the surface spins make an important contribution to the magnetization. This local breaking of the symmetry might lead to changes in the band structure, lattice constant or/and atom coordination. Under these conditions, some surface and/or interface related effects occur, such as surface anisotropy and, under certain conditions, core–surface exchange anisotropy can occur.

2.2.1. No or Magnetically Inert Surface Coatings

Surface effects can lead to a decrease of the magnetization of small particles, for instance oxide nanoparticles, with respect to the bulk value. This reduction has been associated with different mechanisms, such as the existence of a magnetically dead layer on the particle's surface, the existence of canted spins, or the existence of a spin-glass-like behavior of the surface spins.[28] On the other hand, for small metallic nanoparticles, for example cobalt, an enhancement of the magnetic moment with decreasing size was reported as well.[29] Respaud et al. associated this result with a high surface-to-volume ratio, however, without more detailed explanation.

Another surface-driven effect is the enhancement of the magnetic anisotropy, K_{eff}, with decreasing particle size.[29,30] This anisotropy value can exceed the value obtained from the crystalline and shape anisotropy and is assumed to originate from the surface anisotropy. In a very simple approximation, the anisotropy energy of a spherical particle with diameter D, surface area S, and volume V, may be described by one contribution from the bulk and another from the surface: $K_{eff} = K_V + \frac{6}{D}K_S$, where K_V and K_S are the bulk and surface anisotropy energy constants, respectively. Bøder et al.[30] have shown that K_{eff} changes when the surfaces are modified or adsorb different molecules, which explains very well the contribution of the surface anisotropy to K_{eff}.

For uncoated antiferromagnetic nanoparticles, weak ferromagnetism can occur at low temperatures (Figure 1 f), which has been attributed to the existence of uncompensated surface spins of the antiferromagnet.[31–34] Since this situation effectively corresponds to the presence of a ferromagnet in close proximity to an antiferromagnet, additional effects, such as exchange bias, can result (see Section 2.2.2).

However, only in some cases can a clear correlation between the surface coating and the magnetic properties be established. For example, a silica coating is used to tune the magnetic properties of nanoparticles, since the extent of dipolar coupling is related to the distance between particles and this in turn depends on the thickness of the inert silica shell.[35] A thin silica layer will separate the particles, thereby preventing a cooperative switching which is desirable in magnetic storage data.

In other cases, the effect of the coating is less clear. A precious-metal layer around the magnetic nanoparticles will have an influence on the magnetic properties. For example, it was shown that gold-coated cobalt nanoparticles have a lower magnetic anisotropy than uncoated particles, whereas gold

coating of iron particles enhances the anisotropy, an effect which was attributed to alloy formation with the gold.[36] Hormes et al. also discussed the influence of various coatings (e.g., Cu, Au) on the magnetic properties of cobalt nanoparticles, and came to the conclusion that a complex interplay between particle core and coating determines the properties, and tuning may therefore be difficult.[37]

Organic ligands, used to stabilize the magnetic nanoparticles, also have an influence on their magnetic properties, that is, ligands can modify the anisotropy and magnetic moment of the metal atoms located at the surface of the particles.[36] As Paulus and co-workers reported, cobalt colloidal particles stabilized with organic ligands show a reduction of the magnetic moment and a large anisotropy.[36] Leeuwen et al. proposed that surface-bonded ligands lead to the quenching of the surface magnetic moments, resulting in the reduction of magnetization.[38] In the case of nickel nanoparticles, Cordente et al. have demonstrated that donor ligands, such as amines, do not alter the surface magnetism but promote the formation of rods, whereas the use of trioctylphosphine oxide leads to a reduction in the magnetization of the particles.[39] Overall, it must be concluded that the magnetic response of a system to an inert coating is rather complex and system specific, so that no firm correlations can be established at present.

2.2.2. *Magnetic Coatings for Magnetic Nanoparticles*

A magnetic coating on a magnetic nanoparticle usually has a dramatic influence on the magnetic properties. The combination of two different magnetic phases will lead to new magnetic nanocomposites, with many possible applications. The most striking feature which takes place when two magnetic phases are in close contact is the exchange bias effect. A recent review of exchange bias in nanostructured systems is given by Nogués et al.[40]

The exchange coupling across the interface between a ferromagnetic core and an antiferromagnetic shell or vice versa, causes this effect. Exchange bias is the shift of the hysteresis loop along the field axis in systems with ferromagnetic (FM)–antiferromagnetic (AFM) interfaces (Figure 1e). This shift is induced by a unidirectional exchange anisotropy created when the system is cooled below the Néel temperature of the antiferromagnet. This exchange coupling can provide an extra source of anisotropy leading to magnetization stabilization. The exchange bias effect was measured for the first time in cobalt nanoparticles surrounded by an antiferromagnetic CoO layer. There are numerous systems where the exchange bias has been observed, and some of the most investigated systems are: ferromagnetic nanoparticles coated with their antiferromagnetic oxides (e.g., Co/CoO, Ni/NiO), nitrides (Fe–Fe_2N), and sulfides (Fe–FeS), ferrimagnetic–antiferromagnetic (Fe_3O_4–CoO), or ferrimagnetic–ferromagnetic (TbCo–$Fe_{20}Ni_{80}$) nanoparticles.

Recently, single-domain pure antiferromagnetic nanoparticles have shown an exchange-bias effect arising from uncompensated spins on the surface. This reveals a complicated surface spin structure which is responsible for the occurrence of a weak ferromagnetism (Figure 1f), the exchange bias effect, and the so-called training effect.[41] The training effect represents a reduction of the exchange bias field upon subsequent field cycling.

Metallic particles embedded in a matrix are interesting systems of magnetic-coated particles. Skumryev et al. have demonstrated the role of the matrix in establishing the magnetic response of small particles.[42] The magnetic behavior of the isolated 4-nm Co particles with a CoO shell changes dramatically when, instead of being embedded in a paramagnetic matrix, they are embedded in an antiferromagnetic matrix. The blocking temperature of Co particles embedded in an Al_2O_3 or C matrix was around 10 K, but by putting them in a CoO matrix, they remain ferromagnetic up to 290 K. Thus, the coupling of the ferromagnetic particles with an antiferromagnetic matrix is a source of a large additional anisotropy.

Exchange biased nanostructures have found applications in many fields, such as permanent magnets (Figure 1c), recording media, and spintronics. A new approach to produce high-performance permanent magnets is the combination of a soft magnetic phase (easily magnetized), such as Fe_3Pt, and a hard magnetic phase (difficult to magnetize and thus having high coercivity), such as Fe_3O_4 which interact through magnetic exchange coupling.[43]

The right choice of ferromagnetic and antiferromagnetic components can provide a structure suitable for use as a recording medium. The exchange coupling can supply the extra anisotropy which is needed for magnetization stabilization, thus generating magnetically stable particles.

Another interesting aspect related to a magnetic coating is given by the bimagnetic core–shell structure, where both the core and the shell, are strongly magnetic (e.g., FePt/$CoFe_2O_4$).[44] These bimagnetic core–shell nanoparticles will allow a precise tailoring of the magnetic properties through tuning the dimensions of the core and shell, which selectively controls the anisotropy and the magnetization.

Some important aspects should be emphasized. The magnetic behavior of an assembly of nanoparticles is a result of both the intrinsic properties of the particles and the interactions among them. The distribution of the sizes, shapes, surface defects, and phase purity are only a few of the parameters influencing the magnetic properties, which makes the investigation of the magnetism in small particles very complicated. One of the great challenges remains the manufacturing of an assembly of monodisperse particles, with well-defined shape, a controlled composition, ideal chemical stability, tunable interparticle separations, and a functionalizable surface. Such particles will tremendously facilitate the discrimination between finite-size effects, interparticle interactions, and surface effects. Thus, the synthesis of magnetic nanoparticles with well-controlled characteristics is a very important task, which will be described in more detail in the next sections.

3. Synthesis of Magnetic Nanoparticles

Magnetic nanoparticles have been synthesized with a number of different compositions and phases, including iron

oxides, such as Fe_3O_4 and γ-Fe_2O_3,[45–47] pure metals, such as Fe and Co,[48,49] spinel-type ferromagnets, such as $MgFe_2O_4$, $MnFe_2O_4$, and $CoFe_2O_4$,[50,51] as well as alloys, such as $CoPt_3$ and FePt.[52,53] In the last decades, much research has been devoted to the synthesis of magnetic nanoparticles. Especially during the last few years, many publications have described efficient synthetic routes to shape-controlled, highly stable, and monodisperse magnetic nanoparticles. Several popular methods including co-precipitation, thermal decomposition and/or reduction, micelle synthesis, hydrothermal synthesis, and laser pyrolysis techniques can all be directed at the synthesis of high-quality magnetic nanoparticles. Instead of compiling all this literature which would by far exceed the scope of this review, we try to present typical and representative examples for the discussion of each synthetic pathway and the corresponding formation mechanism.

3.1. Co-Precipitation

Co-precipitation is a facile and convenient way to synthesize iron oxides (either Fe_3O_4 or γ-Fe_2O_3) from aqueous Fe^{2+}/Fe^{3+} salt solutions by the addition of a base under inert atmosphere at room temperature or at elevated temperature. The size, shape, and composition of the magnetic nanoparticles very much depends on the type of salts used (e.g. chlorides, sulfates, nitrates), the Fe^{2+}/Fe^{3+} ratio, the reaction temperature, the pH value and ionic strength of the media. With this synthesis, once the synthetic conditions are fixed, the quality of the magnetite nanoparticles is fully reproducible. The magnetic saturation values of magnetite nanoparticles are experimentally determined to be in the range of 30–50 emu g^{-1}, which is lower than the bulk value, 90 emu g^{-1}. Magnetite nanoparticles are not very stable under ambient conditions, and are easily oxidized to maghemite or dissolved in an acidic medium. Since maghemite is a ferrimagnet, oxidation is the lesser problem. Therefore, magnetite particles can be subjected to deliberate oxidation to convert them into maghemite. This transformation is achieved by dispersing them in acidic medium, then addition of iron(III) nitrate. The maghemite particles obtained are then chemically stable in alkaline and acidic medium.

However, even if the magnetite particles are converted into maghemite after their initial formation, the experimental challenge in the synthesis of Fe_3O_4 by co-precipitation lies in control of the particle size and thus achieving a narrow particle size distribution. Since the blocking temperature depends on particle size, a wide particle size distribution will result in a wide range of blocking temperatures and therefore non-ideal magnetic behavior for many applications. Particles prepared by co-precipitation unfortunately tend to be rather polydisperse. It is well known that a short burst of nucleation and subsequent slow controlled growth is crucial to produce monodisperse particles. Controlling these processes is therefore the key in the production of monodisperse iron oxide magnetic nanoparticles.

Recently, significant advances in preparing monodisperse magnetite nanoparticles, of different sizes, have been made by the use of organic additives as stabilization and/or reducing agents. For example, magnetite nanoparticles with sizes of 4–10 nm can be stabilized in an aqueous solution of 1 wt% polyvinlyalcohol (PVA). However, when using PVA containing 0.1 mol% carboxyl groups as the stabilizing agent, magnetite nanoparticles in the form of chainlike clusters precipitate.[54] This result indicates that the selection of a proper surfactant is an important issue for the stabilization of such particles. Size-tunable maghemite nanoparticles were prepared by initial formation of magnetite in the presence of the trisodium salt of citric acid, in an alkaline medium, and subsequent oxidation at 90 °C for 30 min by iron(III) nitrate. The particle sizes can be varied from 2 to 8 nm by adjusting the molar ratio of citrate ions and metal ions (Fe^{2+} and Fe^{3+}).[55] The effects of several organic anions, such as carboxylate and hydroxy carboxylate ions, on the formation of iron oxides or oxyhydroxides have been studied extensively.[56–58] The formation of surface complexes requires both deprotonated carboxy and deprotonated α-hydroxy groups.[59] Recent studies showed that oleic acid is the best candidate for the stabilization of Fe_3O_4.[60,61] The effect of organic ions on the formation of metal oxides or oxyhydroxides can be rationalized by two competing mechanisms. Chelation of the metal ions can prevent nucleation and lead to the formation of larger particles because the number of nuclei formed is small and the system is dominated by particle growth. On the other hand, the adsorption of additives on the nuclei and the growing crystals may inhibit the growth of the particles, which favors the formation of small units.

3.2. Thermal Decomposition

Inspired by the synthesis of high-quality semiconductor nanocrystals and oxides in non-aqueous media by thermal decomposition,[62–64] similar methods for the synthesis of magnetic particles with control over size and shape have been developed. Monodisperse magnetic nanocrystals with smaller size can essentially be synthesized through the thermal decomposition of organometallic compounds in high-boiling organic solvents containing stabilizing surfactants.[51,65,66] The organometallic precursors include metal acetylacetonates, $[M(acac)_n]$, (M = Fe, Mn, Co, Ni, Cr; $n = 2$ or 3, acac = acetylacetonate), metal cupferronates $[M^xCup_x]$ (M = metal ion; Cup = *N*-nitrosophenylhydroxylamine, $C_6H_5N(NO)O$-),[67] or carbonyls.[68] Fatty acids,[69] oleic acid,[70] and hexadecylamine[71] are often used as surfactants. In principle, the ratios of the starting reagents including organometallic compounds, surfactant, and solvent are the decisive parameters for the control of the size and morphology of magnetic nanoparticles. The reaction temperature, reaction time, as well as aging period may also be crucial for the precise control of size and morphology.

If the metal in the precursor is zerovalent, such as in carbonyls, thermal decomposition initially leads to formation of the metal, but two-step procedures can be used to produce oxide nanoparticles as well. For instance, iron pentacarbonyl can be decomposed in a mixture of octyl ether and oleic acid at 100 °C, subsequent addition of trimethylamine oxide $(CH_3)_3NO$ as a mild oxidant at elevated temperature, results

in formation of monodisperse γ-Fe_2O_3 nanocrystals with a size of approximately 13 nm.[72] Decomposition of precursors with cationic metal centers leads directly to the oxides, that is, to Fe_3O_4, if $[Fe(acac)_3]$ is decomposed in the presence of 1,2-hexadecanediol, oleylamine, and oleic acid in phenol ether.[47,73] Peng and co-workers reported a general decomposition approach for the synthesis of size- and shape-controlled magnetic oxide nanocrystals based on the pyrolysis of metal fatty acid salts in non-aqueous solution.[69] The reaction system was generally composed of the metal fatty acid salts, the corresponding fatty acids (decanoic acid, lauric acid, myristic acid, palmitic acid, oleic acid, stearic acid), a hydrocarbon solvent (octadecene (ODE), n-eicosane, tetracosane, or a mixture of ODE and tetracosane), and activation reagents. Nearly monodisperse Fe_3O_4 nanocrystals, with sizes adjustable over a wide size range (3–50 nm) could be synthesized, with controlled shapes, including dots and cubes, as representatively shown in Figure 2. This method

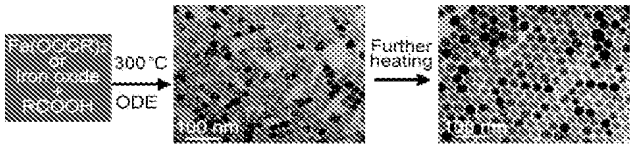

Figure 2. The formation of Fe_3O_4 nanocrystals. The middle and right panels are TEM images of the as-synthesized nanocrystals taken at different reaction times. Reproduced with kind permission from ref. [69].

was successfully generalized for the synthesis of other magnetic nanocrystals, such as Cr_2O_3, MnO, Co_3O_4, and NiO. The size and shape of the nanocrystals could be controlled by variation of the reactivity and concentration of the precursors. The reactivity was tuned by changing the chain length and concentration of the fatty acids. Generally, the shorter the chain length, the faster the reaction rate is. Alcohols or primary amines could be used to accelerate the reaction rate and lower the reaction temperature.

Hyeon and co-workers[51] have also used a similar thermal decomposition approach for the preparation of monodisperse iron oxide nanoparticles. They used nontoxic and inexpensive iron(III) chloride and sodium oleate to generate an iron oleate complex in situ which was then decomposed at temperatures between 240 and 320 °C in different solvents, such as 1-hexadecene, octyl ether, 1-octadecene, 1-eicosene, or trioctylamine. Particle sizes are in the range of 5–22 nm, depending on the decomposition temperature and aging period. In this synthesis, aging was found to be a necessary step for the formation of iron oxide nanoparticles. The nanoparticles obtained are dispersible in various organic solvents including hexane and toluene. However, it is unclear whether the particles can also be dispersed in water. The same group found that sequential decomposition of iron pentacarbonyl and the iron oleate complex at different temperature results in the formation of monodisperse iron nanoparticles (6–15 nm) which can be further oxidized to magnetite.[74] The overall process is similar to seed-mediated growth, which can be explained by the classical LaMer mechanism. That is, a short burst of nucleation from a supersaturated solution is followed by the slow growth of particles without any significant additional nucleation, thereby achieving a complete separation of nucleation and growth.[75] In Hyeon's synthesis, the thermal decomposition of iron pentacarbonyl at relatively low temperature induces nucleation, and the decomposition of the iron oleate complex at a higher temperature leads to growth. The above-mentioned nanoparticles are dispersible in organic solvents. However, water-soluble magnetic nanoparticles are more desirable for applications in biotechnology. For that purpose, a very simple synthesis of water-soluble magnetite nanoparticles was reported recently. Using $FeCl_3 \cdot 6H_2O$ as iron source and 2-pyrrolidone as coordinating solvent, water soluble Fe_3O_4 nanocrystals were prepared under reflux (245 °C).[76] The mean particles size can be controlled at 4, 12, and 60 nm, respectively, when the reflux time is 1, 10, and 24 h. With increasing reflux time, the shapes of the particles changed from spherical at early stage to cubic morphologies for longer times. More recently, the same group developed a one-pot synthesis of water-soluble magnetite nanoparticles prepared under similar reaction conditions by the addition of α,ω-dicarboxyl-terminated poly(ethylene glycol) as a surface-capping agent.[77] These nanoparticles can potentially be used as magnetic resonance imaging contrast agents for cancer diagnosis.

The thermal-decomposition method is also used to prepare metallic nanoparticles. The advantage of metallic nanoparticles is their larger magnetization compared to metal oxides, which is especially interesting for data-storage media. Metallic iron nanoparticles were synthesized by thermal decomposition of $[Fe(CO)_5]$ and in the presence of polyisobutene in decalin under nitrogen atmosphere at 170 °C.[78] The particle size can be adjusted from 2 to 10 nm, with a polydispersity of approximately 10%, depending on the ratio of $Fe(CO)_5$/polyisobutene. The thickness of the polymer layer around the iron nanoparticles was about 7.0 nm. However, these iron particles can still be easily oxidized by exposure to air, as revealed by the susceptibility measurements. This leads to a slight increase of particle sizes by a factor of approximately 1.3. Chaudret and co-workers reported a synthesis of iron nanocubes by the decomposition of $[Fe\{N[Si(CH_3)_3]_2\}_2]$ with H_2 in the presence of hexadecylamine and oleic acid or hexadecylammonium chloride at 150 °C.[79] By variation of the relative concentrations of amine and acid ligand, the size (edge-length) of the nanocubes can be slightly varied from 7 to 8.3 nm with the interparticle space of 1.6 nm to 2 nm, respectively. These nanocubes can assemble into extended crystalline superlattices with their crystallographic axes aligned.

In the synthesis of cobalt nanoparticles by the thermal-decomposition method, both their shape and size can be controlled.[80] Alivisatos and co-workers reported the synthesis of cobalt nanodisks by the thermal decomposition of a cobalt carbonyl precursor.[49,81] Chaudret and co-workers described the synthesis of cobalt nanorods[82,83] and nickel nanorods[39] from the high-temperature reduction of non-carbonyl organometallic complexes. For instance, monodis-

perse ferromagnetic cobalt nanorods were synthesized through the decomposition of $[Co(\eta^3\text{-}C_8H_{13})(\eta^4\text{-}C_8H_{12})]$ under H_2 in anisole at 150 °C in the presence of a mixture of hexadecylamine and a fatty acid, such as lauric acid, octanoic acid, or stearic acid. As seen in Figure 3, the diameter and length of the cobalt nanorods are variable by selecting different acids.[83]

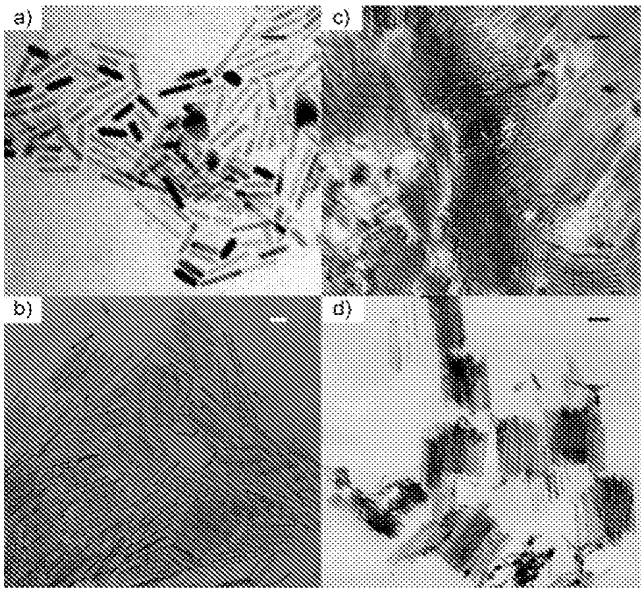

Figure 3. TEM micrographs of nanorods synthesized using hexadecylamine and a) octanoic acid, b) lauric acid, and c, d) stearic acid. The specimen used for the TEM in (c) was prepared by ultramicrotomy. Scale bar: 30 nm. Reproduced from ref. [83].

Air-stable magnetic nanoparticles are very attractive in terms of easy handling and application under oxidizing conditions. Bönnemann et al. reported the synthesis of air-stable "monodisperse" colloidal cobalt nanoparticles by the thermolysis of $[Co_2(CO)_8]$ in the presence of aluminum alkyl compounds.[84] By varying the alkyl chain length of the organo aluminum compounds, the sizes of the Co particles can be tuned in the range of 3–11 nm. It was found that gentle surface oxidation of the cobalt nanoparticles with synthetic air was necessary and crucial to obtain air-stable particles. Without this oxidation step, saturation magnetization of the Co^0 particles decays rapidly when exposed to air after the peptization with the surfactant Korantin SH.

Magnetic alloys have many advantages, such as high magnetic anisotropy, enhanced magnetic susceptibility, and large coercivities.[85] Beside $CoPt_3$ and FePt,[52,53] metal phosphides are currently of great scientific interest in materials science and chemistry.[86,87] For example, hexagonal iron phosphide and related materials have been intensively studied for their ferromagnetism, magnetoresistance, and magnetocaloric effects.[88,89] Recently, Brock and co-workers have synthesized FeP and MnP nanoparticles from the reaction of iron(III) acetylacetonate and manganese carbonyl, respectively, with tris(trimethylsilyl)phosphane at high temperatures.[90,91] Very recently, antiferromagnetic FeP nanorods were prepared by the thermal decomposition of a precursor/surfactant mixture solution.[92] In addition, synthesis of discrete iron phosphide (Fe_2P) nanorods from the thermal decomposition of continuously supplied iron pentacarbonyl in trioctylphosphane using a syringe pump was reported.[93]

3.3. Microemulsion

A microemulsion is a thermodynamically stable isotropic dispersion of two immiscible liquids, where the microdomain of either or both liquids is stabilized by an interfacial film of surfactant molecules.[94] In water-in-oil microemulsions, the aqueous phase is dispersed as microdroplets (typically 1–50 nm in diameter) surrounded by a monolayer of surfactant molecules in the continuous hydrocarbon phase. The size of the reverse micelle is determined by the molar ratio of water to surfactant.[95] By mixing two identical water-in-oil microemulsions containing the desired reactants, the microdroplets will continuously collide, coalesce, and break again, and finally a precipitate forms in the micelles.[4] By the addition of solvent, such as acetone or ethanol, to the microemulsions, the precipitate can be extracted by filtering or centrifuging the mixture. In this sense, a microemulsion can be used as a nanoreactor for the formation of nanoparticles.

Using the microemulsion technique, metallic cobalt, cobalt/platinum alloys, and gold-coated cobalt/platinum nanoparticles have been synthesized in reverse micelles of cetyltrimethlyammonium bromide, using 1-butanol as the cosurfactant and octane as the oil phase.[96] MFe_2O_4 (M: Mn, Co, Ni, Cu, Zn, Mg, or Cd, etc.) are among the most important magnetic materials and have been widely used for electronic applications. Spinel ferrites can be synthesized in microemulsions and inverse micelles. For instance, $MnFe_2O_4$ nanoparticles with controllable sizes from about 4–15 nm are synthesized through the formation of water-in-toluene inverse micelles with sodium dodecylbenzenesulfonate (NaDBS) as surfactant.[97] This synthesis starts with a clear aqueous solution consisting of $Mn(NO_3)_2$ and $Fe(NO_3)_3$. A NaDBS aqueous solution is added to the metal salt solution, subsequent addition of a large volume of toluene forms reverse micelles. The volume ratio of water and toluene determines the size of the resulting $MnFe_2O_4$ nanoparticles. Woo et al. reported that iron oxide nanorods can be fabricated through a sol–gel reaction in reverse micelles formed from oleic acid and benzyl ether, using $FeCl_3 \cdot 6H_2O$ as iron source and propylene oxide as a proton scavenger.[98] The phase of the nanorods can be controlled by variation of the reaction temperature, atmosphere, and hydration state of the gels during reflux or heating in tetralin. A cobalt ferrite fluid was prepared by the reaction of methylamine and in-situ formed cobalt and iron dodecyl sulfate which were made by mixing an aqueous solution of sodium dodecyl sulfate either with iron chloride or with cobalt acetate solution.[99] The size of the cobalt ferrite particles decreases with decreasing total reactant concentration and increasing sodium dodecyl sulfate concentration. The average size of the particles can be varied

from 2 to 5 nm. However, the polydispersity is rather high at 30–35%.

Using the microemulsion technique, nanoparticles can be prepared as spheroids, but also with an oblong cross section or as tubes.[100] Although many types of magnetic nanoparticles have been synthesized in a controlled manner using the microemulsion method, the particle size and shapes usually vary over a relative wide range. Moreover, the working window for the synthesis in microemulsions is usually quite narrow and the yield of nanoparticles is low compared to other methods, such as thermal decomposition and co-precipitation. Large amounts of solvent are necessary to synthesize appreciable amounts of material. It is thus not a very efficient process and also rather difficult to scale-up.

3.4. Hydrothermal Synthesis

Under hydrothermal conditions a broad range of nanostructured materials can be formed. Li et al. reported a generalized hydrothermal method for synthesizing a variety of different nanocrystals by a liquid–solid–solution reaction. The system consists of metal linoleate (solid), an ethanol–linoleic acid liquid phase, and a water–ethanol solution at different reaction temperatures under hydrothermal conditions.[101] As illustrated in Figure 4, this strategy is based on a general phase transfer and separation mechanism occurring at the interfaces of the liquid, solid, and solution phases present during the synthesis. As an example, Fe_3O_4 and $CoFe_2O_4$ nanoparticles can be prepared in very uniform sizes of about 9 and 12 nm, respectively (see Figure 4). Li et al. also reported a synthesis of monodisperse, hydrophilic, single-crystalline ferrite microspheres by hydrothermal reduction.[102] A mixture, consisting of $FeCl_3$, ethylene glycol, sodium acetate, and polyethylene glycol, was stirred vigorously to form a clear solution, then sealed in a Teflon-lined stainless-steel autoclave, and heated to and maintained at 200°C for 8–72 h. In this way, monodisperse ferrite spheres were obtained with tunable sizes in the range of 200–800 nm. Li et al. skillfully used the multicomponent reaction mixtures, including ethylene glycol, sodium acetate, and polyethylene glycol, to direct the synthesis: Ethylene glycol was used as a high-boiling-point reducing agent, which was known from the polyol process to produce monodisperse metal or metal oxide

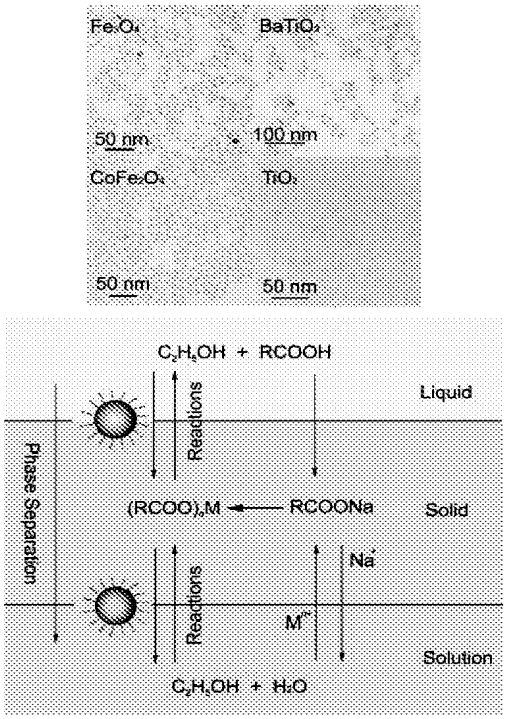

Figure 4. Top: TEM images of Magnetic and dielectric nanocrystals: Fe_3O_4 (9.1 ± 0.8 nm; Fe^{2+}:Fe^{3+}, 1:2; 160°C), $CoFe_2O_4$ (11.5 ± 0.6 nm; Co^{2+}:Fe^{2+}, 1:2; 180°C), $BaTiO_3$ (16.8 ± 1.7 nm; 180°C), TiO_2 (4.3 ± 0.2 nm; 180°C). Bottom: The liquid-solid-solution (LSS) phase-transfer synthetic strategy. Reproduced with kind permission from ref. [101].

nanoparticles; sodium acetate as electrostatic stabilizer to prevent particle agglomeration, and polyethylene glycol as a surfactant against particle agglomeration. Although the mechanism is not fully clear to date, the multicomponent approach seems to be powerful in directing the formation of desired materials.

The advantages and disadvantages of the four above-mentioned synthetic methods are briefly summarized in Table 3. In terms of simplicity of the synthesis, co-precipitation is the preferred route. In terms of size and morphology control of the nanoparticles, thermal decomposition seems the best method developed to date. As an alternative,

Table 3: Summary comparison of the synthetic methods.

Synthetic method	Synthesis	Reaction temp. [°C]	Reaction period	Solvent	Surface-capping agents	Size distribution	Shape control	Yield
co-precipitation	very simple, ambient conditions	20–90	minutes	water	needed, added during or after reaction	relatively narrow	not good	high/ scalable
thermal decomposition	complicated, inert atmosphere	100–320	hours–days	organic compound	needed, added during reaction	very narrow	very good	high/ scalable
microemulsion	complicated, ambient conditions	20–50	hours	organic compound	needed, added during reaction	relatively narrow	good	low
hydrothermal synthesis	simple, high pressure	220	hours ca. days	water-ethanol	needed, added during reaction	very narrow	very good	medium

microemulsions can also be used to synthesize monodispersed nanoparticles with various morphologies. However, this method requires a large amount of solvent. Hydrothermal synthesis is a relatively little explored method for the synthesis of magnetic nanoparticles, although it allows the synthesis of high-quality nanoparticles. To date, magnetic nanoparticles prepared from co-precipitation and thermal decomposition are the best studied, and they can be prepared on a large scale.

The colloidal stability of magnetic nanoparticles synthesized by the above-mentioned methods results either from steric or electrostatic repulsion, depending on the stabilizers, such as fatty acids or amines, and the polarity of the solvent used. For instance, magnetite nanoparticles synthesized through co-precipitation were stabilized by repulsive electrostatic forces because the particles are positively charged.[55] However, nanoparticles synthesized by thermal decomposition are, in general, sterically stabilized in an organic solvent by fatty acids or surfactant.[65] In the following section, the colloidal and chemical stability will be discussed.

4. Protection/Stabilization of Magnetic Nanoparticles

Although there have been many significant developments in the synthesis of magnetic nanoparticles, maintaining the stability of these particles for a long time without agglomeration or precipitation is an important issue. Stability is a crucial requirement for almost any application of magnetic nanoparticles. Especially pure metals, such as Fe, Co, and Ni and their metal alloys, are very sensitive to air. Thus, the main difficulty for the use of pure metals or alloys arises from their instability towards oxidation in air, and the susceptibility towards oxidation becomes higher the smaller the particles are. Therefore, it is necessary to develop efficient strategies to improve the chemical stability of magnetic nanoparticles. The most straightforward method seems to be protection by a layer which is impenetrable, so that oxygen can not reach the surface of the magnetic particles. Often, stabilization and protection of the particles are closely linked with each other.

This section, focuses on the strategies for the protection of magnetic nanoparticles against oxidation by oxygen, or erosion by acid or base. All the protection strategies result in magnetic nanoparticles with a core–shell structure, that is, the naked magnetic nanoparticle as a core is coated by a shell, isolating the core against the environment. The applied coating strategies can roughly be divided into two major groups: coating with organic shells, including surfactant and polymers,[103–107] or coating with inorganic components, including silica,[108] carbon,[109] precious metals (such as Ag,[110] Au[111,112]) or oxides, which can be created by gentle oxidation of the outer shell of the nanoparticles, or additionally deposited, such as Y_2O_3.[113] As an alternative, magnetic nanoparticles can also be dispersed/embedded into a dense matrix, typically in polymer, silica, or carbon, to form composites, which also prevents or at least minimizes the agglomeration and oxidation. However, the nanoparticles are then fixed in space relative to each other, which is often not desired. In contrast, individually protected nanocrystals are freely dispersible and stable in a variety of media owing to the protecting shell around them.[114]

4.1. Surface Passivation by Mild Oxidation

A very simple approach to protect the magnetic particles is to induce a controlled oxidation of a pure metal core, a technique long known for the passivation of air-sensitive supported catalysts. This oxidation can be achieved by various methods. For example, Peng et al. developed a method for oxidizing gas-phase nanoparticles by using a plasma-gas-condensation-type cluster deposition apparatus.[115] Boyen et al. demonstrated that very good control over the chemical state of the cobalt nanoparticles was achieved by their exposure to an oxygen plasma.[116] The control of the oxide layer has a tremendous impact on exchange-biased systems, where a well-defined thickness of the ferromagnetic core and the antiferromagnetic shell are desirable. Moreover, a direct correlation of the structure and magnetism in the small particles can be determined. Bönnemann et al. developed a mild oxidation method, using synthetic air to smoothly oxidize the as-synthesized cobalt nanoparticles to form a stable CoO outer layer which can stabilize the cobalt nanoparticles against further oxidation.[84]

4.2. Surfactant and Polymer Coating

Surfactants or polymers are often employed to passivate the surface of the nanoparticles during or after the synthesis to avoid agglomeration. In general, electrostatic repulsion or steric repulsion can be used to disperse nanoparticles and keep them in a stable colloidal state. The best known example for such systems are the ferrofluids which were invented by Papell in 1965.[117] In the case of ferrofluids, the surface properties of the magnetic particles are the main factors determining colloidal stability. The major measures used to enhance the stability of ferrofluids are the control of surface charge[118] and the use of specific surfactants.[119–121] For instance, magnetite nanoparticles synthesized through the co-precipitation of Fe^{2+} and Fe^{3+} in ammonia or NaOH solution are usually negatively charged, resulting in agglomeration. To achieve stable colloids, the magnetite nanoparticle precipitate can be peptized (to disperse a precipitate to form a colloid by adding of surfactant) with aqueous tetramethylammonium hydroxide or with aqueous perchloric acid.[118] The magnetite nanoparticles can be acidified with a solution of nitric acid and then further oxidized to maghemite by iron nitrate. After centrifugation and redispersion in water, a ferrofluid based on positively charged γ-Fe_2O_3 nanoparticles was obtained, since the surface hydroxy groups are protonated in the acidic medium.[122] Commercially, water- or oil-based ferrofluids are available. They are usually stable when the pH value is below 5 (acidic ferrofluid) or over 8 (alkaline ferrofluid).

In general, surfactants or polymers can be chemically anchored or physically adsorbed on magnetic nanoparticles to

form a single or double layer,[123,124] which creates repulsive (mainly as steric repulsion) forces to balance the magnetic and the van der Waals attractive forces acting on the nanoparticles. Thus, by steric repulsion, the magnetic particles are stabilized in suspension. Polymers containing functional groups, such as carboxylic acids, phosphates, and sulfates, can bind to the surface of magnetite.[125] Suitable polymers for coating include poly(pyrrole), poly(aniline), poly(alkylcyanoacrylates), poly(methylidene malonate), and polyesters, such as poly(lactic acid), poly (glycolic acid), poly(ε-caprolactone), and their copolymers.[126–129] Surface-modified magnetic nanoparticles with certain biocompatible polymers are intensively studied for magnetic-field-directed drug targeting, and as contrast agents for magnetic resonance imaging.[130,131]

Chu et al. reported a synthesis of polymer-coated magnetite nanoparticles by a single inverse microemulsion.[132] The magnetite particles were first synthesized in an inverse microemulsion, consisting of water/sodium bis(2-ethylhexyl-sulfosuccinate)/toluene. Subsequently, water, monomers (methacrylic acid and hydroxyethyl methacrylate), cross-linker (*N*,*N*′-methylenebis(acrylamide)), and an initiator (2,2′-azobis(isobutyronitrile)) were added to the reaction mixture under nitrogen, and the polymerization reaction was conducted at 55 °C. After polymerization, the particles were recovered by precipitation in an excess of an acetone/methanol mixture (9:1 ratio). The polymer-coated nanoparticles have superparamagnetic properties and a narrow size distribution at a size of about 80 nm. However, the long-term stability of these polymer-coated nanoparticles was not addressed. Polyaniline can also be used to coat nanosized ferromagnetic Fe_3O_4 by oxidative polymerization in the presence of the oxidant ammonium peroxodisulfate.[133] The nanoparticles obtained are polydisperse (20–30 nm averaged diameter) and have the expected core–shell morphology. Asher et al. reported that single iron oxide particles (ca. 10 nm) can be embedded in polystyrene spheres through emulsion polymerization to give stable superparamagnetic photonic crystals.[134] Polystyrene coating of iron oxide nanoparticles was also achieved by atom transfer radical polymerization.[135,136] For instance, Zhang et al. have used this method for coating $MnFe_2O_4$ nanoparticles with polystyrene, yielding core–shell nanoparticles with sizes below 15 nm. The overall synthetic procedure is schematically shown in Figure 5. $MnFe_2O_4$ nanoparticles (ca. 9 nm) were stirred overnight in aqueous initiator solution, 3-chloropropionic acid, at pH 4.[135] After washing out the excess initiator, air-dried nanoparticles were added to a styrene solution under nitrogen, then xylene, containing CuCl and 4,4′-dinonyl-2,2′-dipyridyl was added. The solution was stirred and kept at 130 °C for 24 h to give the polystyrene coated $MnFe_2O_4$ nanoparticles. When using a free radical polymerization with $K_2S_2O_8$ as the catalyst, predominantly polystyrene particles without a magnetic core were obtained. This result confirms that the surface-grafted initiator is important for the coating of the nanoparticles.

Metallic magnetic nanoparticles, stabilized by single or double layers of surfactant or polymer are not air stable, and are easily leached by acidic solution,[68] resulting in the loss of their magnetization. A thin polymer coating is not a good enough barrier to prevent oxidation of the highly reactive metal particles. Polymer coating is thus not very suitable to protect very reactive magnetic nanoparticles.

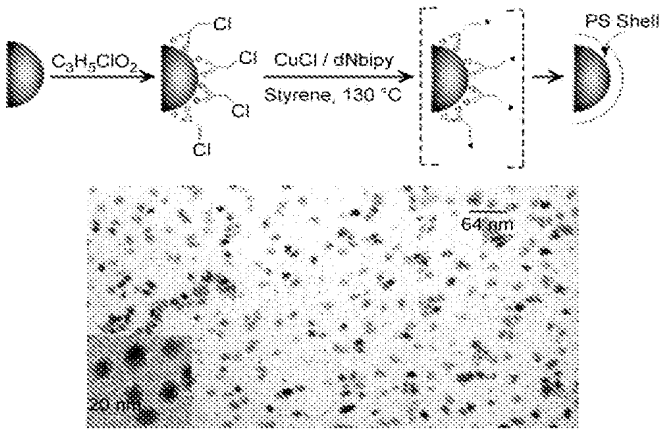

Figure 5. Top: Illustration of the polystyrene coating on $MnFe_2O_4$ by atom-transfer radical polymerization. Polymerization initiators are chemically attached onto the surface of nanoparticles. The modified nanoparticles are then used as macro-initiators in the subsequent polymerization reaction. Bottom: TEM micrographs of approximately 9-nm diameter $MnFe_2O_4$/polystyrene core–shell nanoparticles. Reproduced with kind permission from ref. [135]. dNbipy = 4,4′-dinonyl-2,2′-dipyridyl.

Another drawback of polymer-coated magnetic nanoparticles is the relatively low intrinsic stability of the coating at higher temperature, a problem which is even enhanced by a possible catalytic action of the metallic cores. Therefore, the development of other methods for protecting magnetic nanoparticles against deterioration is of great importance.

4.3. Precious-Metal Coating

Precious metals can be deposited on magnetic nanoparticles through reactions in microemulsion,[137,138] redox transmetalation,[139–141] iterative hydroxylamine seeding,[142] or other methods, to protect the cores against oxidation. Cheon et al. reported a synthesis of platinum-coated cobalt by refluxing cobalt nanoparticle colloids (ca. 6 nm) and [Pt(hfac)$_2$] (hfac = hexafluoroacetylacetonate) in a nonane solution containing $C_{12}H_{25}NC$ as a stabilizer.[139] After 8 h reflux and addition of ethanol and centrifugation, the colloids are isolated from the dark red-black solution in powder form. The TEM images of the platinum-coated cobalt particles with sizes below 10 nm are shown in Figure 6.

These particles are air stable and can be redispersed in typical organic solvents. The reaction byproduct was separated and analyzed as [Co(hfac)$_2$], indicating that the formation of the core–shell structure was driven by redox transmetalation reactions between Co^0 and Pt^{2+}.

Gold seems to be an ideal coating owing to its low reactivity. However, it was found that the direct coating of magnetic particles with gold is very difficult, because of the dissimilar nature of the two surfaces.[143–146] Progress has been made, though, recently. O'Connor and co-workers have synthesized gold-coated iron nanoparticles with about

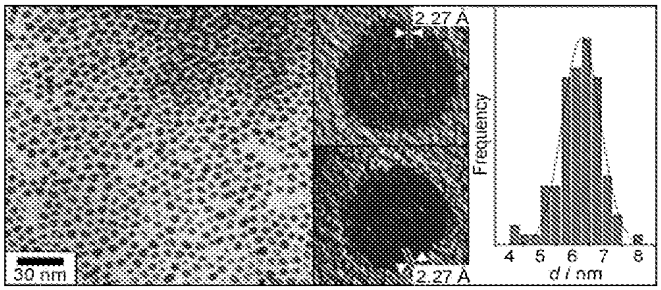

Figure 6. Left: TEM images of $Co_{core}Pt_{shell}$ nanoalloys. In the enlarged images the spacings of the lattice fringes are given which are consistent with the Pt(111) plane. Right: the particle size distribution. Reproduced with kind permission from ref. [139].

11 nm core size and a gold shell of about 2.5 nm thickness.[140] These gold coated iron particles are stable under neutral and acidic aqueous conditions. The coating was achieved by a partial replacement reaction in a polar aprotic solvent. Briefly, a yellow solution of $FeCl_3$, dissolved in 1-methyl-2-pyrrolidinone (NMPO), was added to a dark green NMPO solution containing sodium and naphthalene under intensive stirring at room temperature. Thus, the Fe^{3+} ions were reduced by sodium to form the metallic cores. After removal of sodium chloride by centrifugation, and the addition of 4-benzylpyridine as capping agent at elevated temperature, the iron nanoparticles were coated with gold by the addition of dehydrated $HAuCl_4$ dissolved in NMPO.

Gold-coated iron nanoparticles could also be prepared by a reverse microemulsion method. The inverse micelles were formed with cetyltrimethylammonium bromide (CTAB) as surfactant, 1-butanol as a co-surfactant, and octane as the continuous oil phase. $FeSO_4$ was reduced by $NaBH_4$, then addition of $HAuCl_4$ coated gold on the iron nanoparticles.[111] Zhang et al. reported a new method for the preparation of gold coated iron magnetic core–shell nanoparticles by the combination of wet chemistry and laser irradiation. The synthesized iron nanoparticles and gold powder were irradiated by a laser in a liquid medium to deposit the gold shell.[147] The 18 nm body centered cubic (bcc) iron single domain magnetic cores are covered by a gold shell of partially fused approximately 3-nm-diameter fcc gold nanoparticles. The core–shell particles are superparamagnetic at room temperature with a blocking temperature, T_B, of approximately 170 K. After four months of shelf storage in normal laboratory conditions, their magnetization normalized to iron content was measured to be 210 emu g^{-1}, roughly 96% of the bulk iron value, which indicates the high stability.

Guo et al. have reported a synthesis of gold coated cobalt nanoparticles based on a chemical reduction reaction.[148,149] The cobalt particles were fabricated using 3-(*N*,*N*-dimethyldodecylammonio) propanesulfonate as the surfactant to prevent agglomeration, and lithium triethylhydridoborate as the reducing agent. The cobalt nanoparticles produced were added to $KAuCl_4$ in tetrahydrofuran (THF) solution under ultrasonication and inert atmosphere. The gold shell was deposited on the cobalt nanoparticle through reduction of the Au^{3+} by cobalt surface atoms.

Gold coating of magnetic nanoparticles is especially interesting, since the gold surface can be further functionalized with thiol groups. This treatment allows the linkage of functional ligands which may make the materials suitable for catalytic and optical applications.[150]

4.4. Silica Coating

A silica shell does not only protect the magnetic cores, but can also prevent the direct contact of the magnetic core with additional agents linked to the silica surface thus avoiding unwanted interactions. For instance, the direct attachment of dye molecules to magnetic nanoparticles often results in luminescence quenching. To avoid this problem, a silica shell was first coated on the magnetic core, and then dye molecules were grafted on the silica shell.[151] Silica coatings have several advantages arising from their stability under aqueous conditions (at least if the pH value is sufficiently low), easy surface modification, and easy control of interparticle interactions, both in solution and within structures, through variation of the shell thickness.

The Stöber method and sol–gel processes are the prevailing choices for coating magnetic nanoparticles with silica.[152–156] The coating thickness can be tuned by varying the concentration of ammonium and the ratio of tetraethoxysilane (TEOS) to H_2O. The surfaces of silica-coated magnetic nanoparticles are hydrophilic, and are readily modified with other functional groups.[157] The functionalization could introduce additional functionality, so that the magnetic particles are potentially of use in biolabeling, drug targeting, drug delivery. Previous studies involved the coating of hematite (Fe_2O_3) spindles and much smaller magnetite clusters with silica;[158,159] the oxide cores could subsequently be reduced in the dry state to metallic iron.[160] The advantage of this method is that silica coating was performed on an oxide surface, which easily binds to silica through OH surface groups.

Xia and co-workers have shown that commercially available ferrofluids can be directly coated with silica shells by the hydrolysis of TEOS.[154] A water-based ferrofluid (EMG 340) was diluted with deionized water and 2-propanol. Ammonia solution and various amounts of TEOS were added stepwise to the reaction mixture under stirring. The coating step was allowed to proceed at room temperature for about 3 h under continuous stirring. The coating thickness could be varied by changing the amount of TEOS. Since the iron oxide surface has a strong affinity towards silica, no primer was required to promote the deposition and adhesion of silica. Owing to the negative charges on the silica shells, these coated magnetic nanoparticles are redispersible in water without the need of adding other surfactants. Figure 7 shows the TEM images of silica-coated iron oxide nanoparticles. The images clearly indicate the single-crystalline nature of the iron oxide core and the amorphous nature of the silica shell. Kobayashi et al. described a method for the synthesis of monodisperse, amorphous cobalt nanoparticles coated with silica in aqueous ethanolic solution by using 3-aminopropyl trimethoxysilane and TEOS as the silica precursor.[161] Shi and

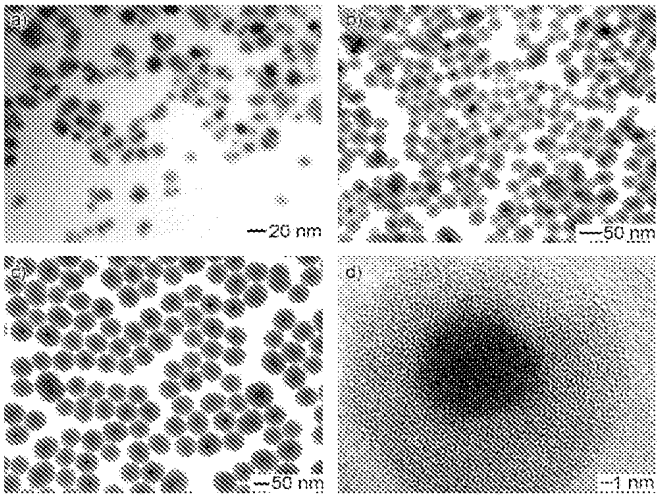

Figure 7. a–c) TEM images of iron oxide nanoparticles coated with silica shells of various thicknesses. The thickness of the silica coating was adjusted by controlling the amount of precursor added to the solution: a) 10, b) 60, and c) 1000 mg of TEOS to 20 mL of 2-propanol. d) HRTEM image of the iron oxide nanoparticle uniformly coated with a 6-nm thin amorphous silica shell. Reproduced with kind permission from ref. [154].

co-workers have prepared uniform magnetic nanospheres (ca. 270 nm) with a magnetic core and a mesoporous-silica shell.[162] The synthesis involved forming a thin and dense silica coating on hematite nanoparticles by the Stöber process, a second coating, the mesoporous silica shell, was added by a simultaneous sol–gel polymerization of TEOS and *n*-octadecyltrimethoxysilane. The hematite core can be reduced to the metallic state by H_2.

Though great progress in the field of silica-coated nanoparticles has been made, the synthesis of uniform silica shells with controlled thickness on the nanometer scale still remains challenging. As an alternative, the microemulsion method was also tried.[163] Homogeneous silica-coated Fe_2O_3 nanoparticles with a silica shell of controlled thickness (1.8–30 nm) were synthesized in a reverse microemulsion.[164] Tartaj et al. reported a synthesis of monodisperse air-stable superparamagnetic α-Fe nanocrystals encapsulated in nanospherical silica particles of 50 nm in diameter. The iron oxide nanoparticles are embedded in silica by the reverse microemulsion technique, the α-Fe is obtained by reduction with hydrogen at 450 °C.[165] Similarly, a reverse micelle microemulsion approach was also reported to coat a layer of silica around spinel ferrite nanoparticles of $CoFe_2O_4$ and $MnFe_2O_4$.[166]

Although metals protected by silica can be synthesized by reduction after synthesis, silica deposition directly on pure metal particles is more complicated because of the lack of OH groups on the metal surface. An additional difficulty for coating metallic nanoparticles, such as iron and cobalt with silica, which has to be overcome, is that iron and cobalt are readily oxidized in the presence of dissolved oxygen. Therefore, it is necessary to use a primer to make the surface "vitreophilic" (glasslike).[167] This chemistry has been used to coat precious metals.[168] Another possibility would be using stable cobalt nanoparticles, passivated by the gentle oxidation method developed by Bönnemann et al.,[84] as starting materials for such silica coating. However, no corresponding report has appeared to date.

Other oxides have rarely been used as protective coatings. Needlelike yttria-coated FeCo nanoparticles were synthesized starting from needlelike YCo-FeOOH nanoparticles, by the combination of a modified carbonate route and electrostatically induced self-assembly methods.[113] The use of yttria as a protective agent has allowed the dehydration temperature of the oxyhydroxides to be increased, decreasing the porosity of samples, and thus improving the magnetic properties of the final metallic particles. The highest value of coercivity (1550 Oe) is obtained for samples containing 20 mol % of cobalt.

From the mentioned examples above, it can be seen that silica coating of magnetic oxide nanoparticles is a fairly controllable process. However, silica is unstable under basic condition, in addition, silica may contain pores through which oxygen or other species could diffuse. Coating with other oxides is much less developed, and therefore alternative methods, especially those which would allow stabilization under alkaline conditions, are needed.

4.5. Carbon Coating

Although to date most studies have focused on the development of polymer or silica protective coatings, recently carbon-protected magnetic nanoparticles are receiving more attention, because carbon-based materials have many advantages over polymer or silica, such as much higher chemical and thermal stability as well as biocompatibility.

Right after the discovery of fullerenes, it was found that carbon-encapsulated metal or metal carbide nanocrystallites can be generated by the Krätschmer arc-discharge process.[169] Since then, many studies have shown that in the presence of metal nanoparticles (Co, Fe, Ni, Cr, Au, etc), graphitized carbon structures, such as carbon nanotubes and carbon onions, are formed under arc-discharge, laser ablation, and electron irradiation.[170–173] The well-developed graphitic carbon layers provide an effective barrier against oxidation and acid erosion. These facts indicate that it is possible to synthesize carbon-coated magnetic nanoparticles, which are thermally stabile and have high stability against oxidation and acid leaching, which is crucial for some applications.[174] Moreover, carbon-coated nanoparticles are usually in the metallic state, and thus have a higher magnetic moment than the corresponding oxides.

Gedanken and co-workers reported a sonochemical procedure that leads to air-stable cobalt nanoparticles.[175] They claim that the high stability arises from the formation of a carbon shell on the nanoparticle surface. However, the particles obtained are rather polydisperse and not very uniform. Johnson et al. describe a simple method to prepare carbon-coated magnetic Fe and Fe_3C nanoparticles by direct pyrolysis of iron stearate at 900 °C under an argon atmosphere.[176] The carbon-coated magnetic nanoparticles obtained are stable up to 400 °C under air. This direct salt-

conversion process is an advantageous single-step process and potentially can be scaled up. However, the nanoparticles produced by this method show a broad size distribution, with a diameter ranging from 20 to 200 nm and the cores are covered with 20 to 80 graphene layers. No information on dispersibility of the nanoparticles was given. Lu et al. have synthesized highly stable carbon-coated cobalt nanoparticles with a size of about 11 nm.[109] The cobalt nanoparticles were coated with furfurly alcohol which was converted first into poly (furfuryl alcohol) and then carbonized to carbon during the pyrolysis, resulting in a stable protection layer against air oxidation, and erosion by strong acids and bases. Interestingly, if CTAB is used as the carbon source, the carbon coating is not perfect and the cobalt core can be leached with acid. Since the imperfect graphite coating is not attacked, graphitic hollow shells were obtained, which may be interesting for use as electrodes. Similar graphitic-carbon-encapsulated cobalt nanoparticles were also prepared through pyrolysis of a composite of metallic cobalt nanoparticles (ca. 8–10 nm) and poly(styrene-*b*-4-vinylphenoxyphthalonitrile).[177] These cobalt-graphitic particles are oxidatively stable and retain their high saturation magnetizations (ca. 95–100 emu g^{-1}) for at least one year under ambient conditions.

We have recently investigated the structure development of cobalt cations chemically adsorbed in an in-house synthesized ion-exchangeable polymer. During pyrolysis, the in-situ formed cobalt nanoparticles continuously catalyze the decomposition of the polymer matrix to form mesoporous graphitic carbon. Cobalt nanoparticles embedded in graphitic carbon were obtained as the final product. Magnetization measurements show that the graphitic carbon/cobalt composites are ferromagnetic, and the cobalt nanoparticles are stable under air for more than 10 months without degradation of their magnetic properties.[178]

Though carbon-coated magnetic nanoparticles have many advantageous properties, such particles are often obtained as agglomerated clusters, owing to the lack of effective synthetic methods, and a low degree of understanding of the formation mechanism. The synthesis of dispersible, carbon-coated nanoparticles in isolated form is currently one of the challenges in this field.

4.6. Matrix-Dispersed Magnetic Nanoparticles

Matrix-dispersed magnetic nanoparticles can be created in a variety of different states: 1) they can be dispersed in a continuous matrix, or 2) they can be present dispersed in a coating on other, larger particles (e.g., core–shell particles prepared by layer-by-layer methods), or 3) they can form agglomerates of individual nanoparticles which are connected through their protective shells.

In the preceding sections we mainly discussed the various coating strategies to protect magnetic nanoparticles against oxidation or erosion in acid or basic environments. In most of the cases discussed, the coated magnetic nanoparticles are present in monodispersed form in solution. However, as discussed for the carbons in Section 4.5, sometimes it is very difficult to avoid agglomeration of the particles. Hence, for some applications this problem could be turned into an advantage, if isolated particles are not mandatory: a relatively easy way of protection is to directly embed the magnetic nanoparticles into a guest matrix to stabilize these particles against oxidation. In this case, the embedded magnetic nanoparticles are randomly distributed in a coherent guest matrix. Nevertheless, such nanoparticles have good stability and retain the desired magnetic properties.

Stoeva et al. have assembled magnetic nanoparticles into a composite structure with a silica core, with Fe_3O_4 and gold as the inner and outer shells, respectively.[179] As illustrated in Figure 8, this approach utilizes positively charged amino-modified SiO_2 particles as templates for the assembly of negatively charged 15-nm superparamagnetic water-soluble Fe_3O_4 nanoparticles. The SiO_2/Fe_3O_4 particles electrostatically attract 1–3 nm gold-nanoparticle seeds that act in a subsequent step as nucleation sites for the formation of a continuous gold shell around the SiO_2/Fe_3O_4 particles upon $HAuCl_4$ reduction. These three-layer magnetic nanoparticles, when functionalized with oligonucleotides, have cooperative DNA binding properties as well as magnetic properties.

Ying et al. reported the synthesis of silica-encapsulated magnetic nanoparticles and quantum dots by the reverse

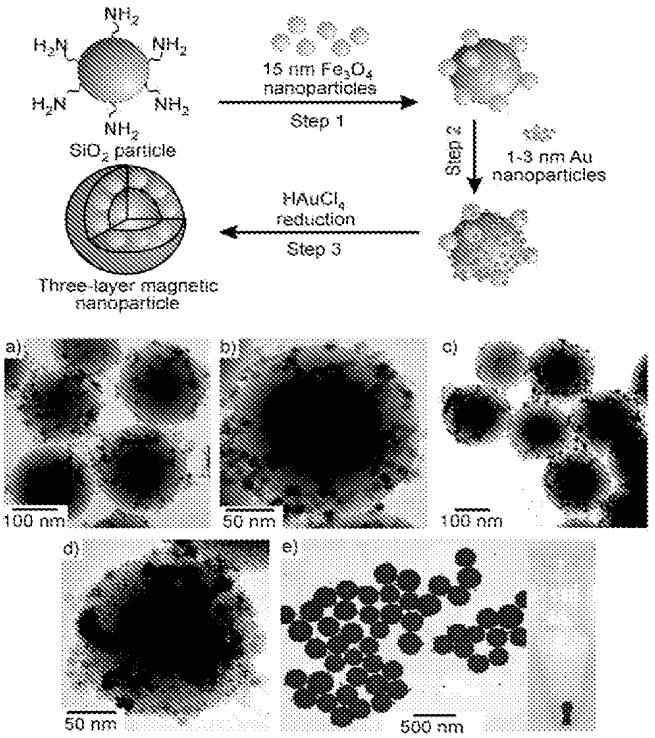

Figure 8. Top: the preparation of three-layer magnetic nanoparticles. Bottom: TEM images of colloids after each synthetic step. a,b) SiO_2 particles covered with silica-primed Fe_3O_4 nanoparticles (SiO_2/Fe_3O_4). c,d) SiO_2 particles covered with silica-primed Fe_3O_4 nanoparticles and heavily loaded with Au nanoparticle seeds ($SiO_2/Fe_3O_4/Au_{seeds}$). e) Three-layer magnetic nanoparticles synthesized in a single-step process from the particles in (c) and (d). Note the uniformity of the gold shell. The inset (right) shows the three-layer magnetic nanoparticles drawn to the wall with a magnet. Reproduced with kind permission from ref. [179].

microemulsion technique.[180] γ-Fe_2O_3 (11.8 nm) and CdSe (3.5 nm) nanoparticles were synthesized separately, and then dispersed in cyclohexane. Then these nanoparticle solutions were introduced into the reverse microemulsion, with subsequent addition of ammonium hydroxide to form a transparent liquid. TEOS was finally added to the reverse microemulsion and allowed to react to completion. The silica-encapsulated γ-Fe_2O_3 and CdSe nanoparticle composites obtained can be redispersed in deionized water or ethanol, although the system is not fully homogeneous. The composites preserve the magnetic properties of γ-Fe_2O_3 and also the optical properties of CdSe, which might be interesting for bioimaging, biosensing, and biolabeling.

Core–shell magnetite particles and hollow spheres were fabricated based on a multistep (layer-by-layer) strategy.[181] The synthetic procedure basically involved coating submicrometer-sized anionic polystyrene lattices with cationic polyelectrolyte PDADMAC (poly(diallyldimethylammonium chloride) which served as anchor sites for adsorbing negatively charged magnetite nanoparticles. As shown in Figure 9, the thickness of the multilayers can be controlled by tuning the number of polyelectrolyte layers deposited between each nanoparticle layer. Electrostatic interactions between the negatively charged nanoparticles and cationic polyelectrolyte were utilized to build up the nanocomposite multilayer structure. Intact hollow magnetic spheres can be obtained by calcinating the core–shell particles at elevated temperature.

Aerosol pyrolysis has also been used for silica coating, but the particles produced are hollow silica spheres with magnetic shells (Figure 10).[182] In brief, TEOS and iron nitrate in the right proportions were dissolved in methanol at a total salt concentration of 1 M. The solution was directed to a first furnace kept at 250 °C to favor the evaporation of the solvent and therefore the precipitation of solute. The solid aerosol was subsequently decomposed in a second furnace, which was held at 500 °C. Finally, the particles obtained were collected with an electrostatic filter. The crucial point in dispersing magnetic nanoparticles in colloidal silica cages is to be careful to select suitable experimental parameters, such as the nature and concentration of precursors and the working temperature.

Carbon nanotubes (CNTs) were used as a guest matrix to be coated with iron oxide nanoparticles by using the polymer wrapping and layer-by-layer assembly techniques.[183] It was demonstrated that the magnetized CNTs can form aligned chains in relatively small external magnetic fields, and would be excellent candidates to be used as building blocks for the fabrication of novel composite materials with a preferential orientation of the magnetic CNTs.

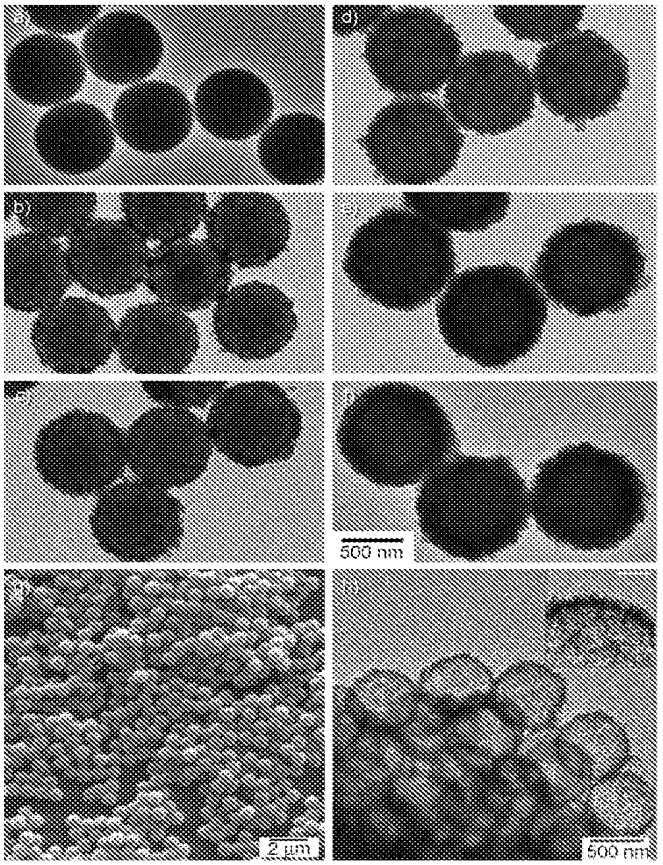

Figure 9. TEM micrographs of a) uncoated polystyrene (PS) lattices and polyelectrolyte (PE_3)-modified PS lattices coated with b) one, c) two, d) three, e) four, and f) five Fe_3O_4 nanoparticle/PE_3 layers. The average diameters of the composite particles are (from (a)–(f)) 650, 700, 770, 820, 890, and 960 nm (the error is approximately $\pm$10 nm). The stepwise increase in the diameter of the coated particles indicates the regular deposition of Fe_3O_4 nanoparticles and polyelectrolytes. The polyelectrolyte interlayer spacing between each Fe_3O_4 nanoparticle layer was PDADMAC/PSS/PDADMAC (i.e., PE_3, PSS = poly(styrene sulfonate)). The scale bar is for all the images. g) SEM image of magnetic hollow spheres prepared by exposing PE_3-coated PS particles to five adsorption cycles of Fe_3O_4 nanoparticles and PDADMAC, followed by calcination at 500 °C. h) TEM image of the same sample showing the hollow nature of the particles. The inset shows the regularity of the wall structure. The scale bar in the inset represents 100 nm. Reproduced with kind permission from ref. [181].

5. Functionalization and Applications of Magnetic Nanoparticles

5.1. Functionalization of Coated Magnetic Nanoparticles

As mentioned above, a protective shell does not only serve to protect the magnetic nanoparticles against degradation, but can also be used for further functionalization with specific components, such as catalytically active species, various drugs, specific binding sites, or other functional groups. The easy separation and controlled placement of these functionalized magnetic nanoparticles by means of an external magnetic field enables their application as catalyst supports, in immobilized enzyme processes,[184] and the construction of magnetically controllable bio-electrocatalytic systems.[185,186]

Salgueiriño-Maceira et al. reported a synthesis of iron oxide nanoparticles, coated with a silica shell that were subsequently functionalized with gold nanoparticles:[187] Aqueous dispersions of the iron oxide magnetic nanoparticles

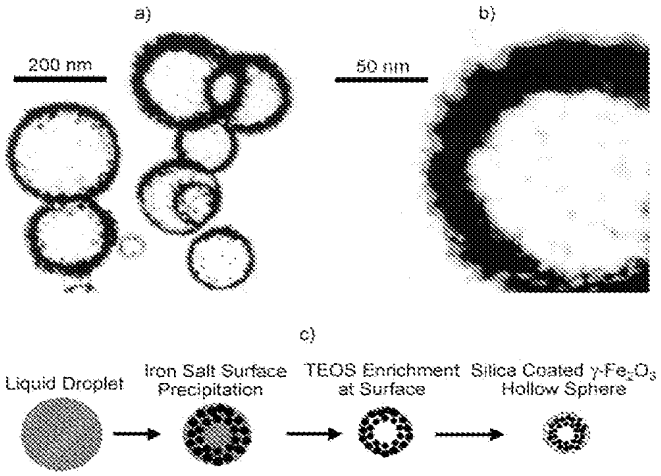

Figure 10. a) TEM picture of silica/iron oxide composites prepared by aerosol pyrolysis. b) Details of a hollow spherical particle showing an outer particle layer mainly consisting (according to TEM microanalyses) of SiO_2. c) The formation mechanism of the silica-coated α-Fe_2O_3 hollow particles. Reproduced with kind permission from ref. [182].

were coated with a silica shell by the Stöber process. The negatively charged silica surface was then sequentially coated with positively-negatively-positively charged polyelectrolyte polymers through electrostatic interactions, followed by the adsorption of citrate-stabilized 15 nm gold nanoparticles. Using those gold particles as seeds, the gold shell was formed onto the magnetic silica spheres step-by-step with reducing aliquots of $HAuCl_4$ and ascorbic acid in aqueous solution. These gold-coated magnetic silica spheres have a strong resonance absorption in the visible and near-infrared range and can be controlled by using an external magnetic field, which makes them very promising in biomedical applications.

The difficulty in preparing functional-polymer magnetic microspheres arises from the magnetic dipolar interaction between adjacent magnetic nanoparticles, this makes it impossible to carry out polymerization on the surface of inorganic magnetic nanoparticles. Recently, a successful example was published for the preparation of thermoresponsive-polymer magnetic microspheres based on cross-linked *N*-isopropylacrylamide (NIPAM) by a colloidal template polymerization. Briefly, magnetic nanoparticles were synthesized by co-precipitation and stabilized by trisodium citrate, then silica coated through the Stöber process. The silica-coated nanoparticles were then functionalized with 3-(trimethoxysily)propyl methacrylate, leading to the formation of C=C bonds on the surface. Finally, a monomer, NIPAM, was polymerized with *N*,*N*′-methylene bisacrylamide as the cross-linker by seed precipitation polymerization in the presence of MPS-modified (MPS = 3-(trimethoxysily)propyl methacrylate) silica-coated nanoparticles as seeds, resulting in the formation of PNIPAM magnetic microspheres, which are thermoresponsive.[188]

Another method for the functionalization of magnetic nanoparticles is ligand exchange, by which the as-synthesized magnetic nanoparticles in an organic phase can be converted into water soluble ones. Rotello and co-workers reported[189] that iron oxide nanoparticles dispersed in a toluene solution can be completely transferred into aqueous solution under stirring with octa(tetramethylammonium)–polyhedral oligomeric silsesquioxane (TMA–POSS). Interestingly, this TMA–POSS exchange strategy can be applied to different monolayer-protected magnetic nanoparticles, such as oleic acid stabilized iron oxide nanoparticles, and oleic acid, oleylamine, or hexadecanediol stabilized FePt nanoparticles. The water-soluble nanoparticles obtained have excellent stability in biologically relevant pH ranges and salt concentrations.

5.2. Applications in Catalysis and Biotechnology

Magnetic nanoparticles with good stability will be of great interest in catalysis and in biotechnology/biomedicine applications. Such magnetic nanoparticles can be very useful to assist an effective separation of catalysts, nuclear waste, biochemical products, and cells.[190–192]

Magnetically driven separations make the recovery of catalysts in a liquid-phase reaction much easier than by cross-flow filtration and centrifugation, especially when the catalysts are in the sub-micrometer size range. Such small and magnetically separable catalysts could combine the advantages of high dispersion and reactivity with easy separation. In terms of recycling expensive catalyst or ligands, immobilization of these active species on magnetic nanoparticles leads to the easy separation of catalysts in a quasi-homogeneous system. Lin et al. have recently synthesized a novel magnetically recoverable heterogenized chiral catalyst through immobilizing a ruthenium(II) complex, $[Ru(binap\text{-}PO_3H_2)(dpen)Cl_2]$ (binap = 2,2′-bis(diphenylphosphino)-1,1′-binaphthyl, dpen = 1,2-diphenylethylenediamine) on magnetite nanoparticles through the phosphonate group.[193] These nanoparticle-supported chiral catalysts were used for enantioselective asymmetric hydrogenation of aromatic ketones with very high enantiomeric excess values of up to 98.0%. The immobilized catalysts were recycled by magnetic decantation and reused up to 14 times without loss of activity and enantioselectivity. These magnetic nanoparticles coupled with chiral catalysts are more accessible to the reactants because of their small size, and are to some extent similar to homogeneous asymmetric catalysts.

Magnetic nanoparticles with core–shell structure may enable the development of a new type of catalyst. The shell consists of the catalytically active species, and the magnetic core can act as anchor to separate and recycle the catalyst. As an example, core–shell-type cobalt–platinum nanoparticles have been prepared by a redox transmetalation reaction between $[Pt(hfac)_2]$ and cobalt nanoparticles.[139,194] The platinum forms a shell around the cobalt core and the shell surface is stabilized by dodecyl isocyanide capping molecules. The core–shell structures are superparamagnetic at room temperature. Such a catalyst has the advantage of economically using the platinum atoms, because only the outer atoms are accessible for the reagents, and the magnetic cobalt core plays a critical role in the separation and recycling of the catalyst. This catalyst is effective for the hydrogenation of

unsaturated organic molecules under mild conditions. If the magnetic species is intrinsically catalytically active for certain reactions, this magnetic catalyst will advantageously combine both the catalytic and the separation function. Thus, iron nanoparticles stabilized by 1,6-bis(diphenylphosphino)hexane or polyethylene glycol exhibit high activity for the cross-coupling of aryl Grignard reagents with primary and secondary alkyl halides bearing β-hydrogen atoms. This catalyst has also proven to be effective in a tandem ring-closing/cross-coupling reaction.[195]

Lu et al. have developed a pathway to synthesize high-surface-area magnetically separable catalysts based on carbon-coated magnetic cobalt nanoparticles (ca. 11 nm in size).[2] Ordered mesoporous silica (SBA-15) was first infiltrated with furfuryl alcohol. After polymerization, the pore system of the silica template was blocked by polyfurfuryl alcohol. In this case the cobalt nanoparticles can be spatially selectively deposited on the external surface of the silica/polymer composite. A coating strategy was employed to protect the cobalt nanoparticles from corrosive media and high-temperature sintering. For this coating small amounts of a carbon precursor were used to cover the cobalt nanoparticles. Pyrolysis resulted in encapsulation of the cobalt nanoparticles by a thin (about 1 nm thick) layer of graphitic carbon, and simultaneously, the polyfurfuryl alcohol, filling the silica pore system, was converted into carbon. After leaching out the silica template, the carbon obtained is superparamagnetic and has a fully accessible pore system, which is available to be functionalized with, for instance, catalytically active species, such as palladium (Figure 11). Such carbon-supported palladium catalysts show high activity and stability in the hydrogenation of octane, and, more importantly, are easily separated by applying a magnetic field. Related work has been carried out on a mesoporous silica decorated with carbon-coated magnetic nanoparticles which was synthesized by a reversible pore blocking and opening strategy.[196] Magnetic nanoparticles were deposited on the external surface of the support, thus leaving the pore system unobstructed for further functionalization.

Magnetically separable mesoporous carbons constructed from mesocellular carbon and Fe/Fe_3O_4 core–shell ferromagnetic nanoparticles (approximately 30 nm in size) show good electron conductivity, large pore size, and large pore volume. After the immobilization of enzymes (glucose oxidase) these particles can be used as magnetically switchable bio-electrocatalytic systems.[197] Hyeon and co-workers have also tried to synthesize monodisperse magnetite nanocrystals and CdSe/ZnS quantum dots both embedded in mesoporous silica spheres. These mesoporous silica spheres were applied to the uptake and controlled release of ibuprofen drugs. The release rate can be controlled by the surface properties of mesoporous silica spheres.[198]

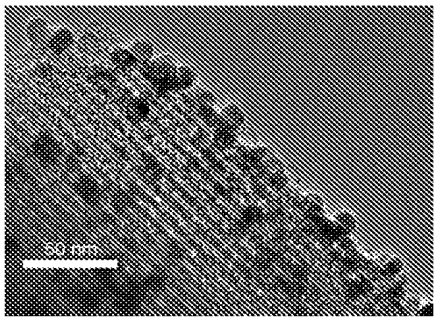

Figure 11. Ordered mesoporous carbon, decorated with superparamagnetic 11 nm sized Co nanoparticles protected by an approximately 1-nm thick carbon shell. The material can be used as magnetically separable sorbent or catalyst support. Reproduced with kind permission from ref. [2].

In biotechnology and biomedicine, magnetic separation can be used as a quick and simple method for the efficient and reliable capture of specific proteins or other biomolecules. Most particles currently used are superparamagnetic, meaning that they can be magnetized with an external magnetic field and immediately redispersed once the magnet is removed. Magnetic iron oxide nanoparticles grafted with dopamine have been used for protein separation.[199] The dopamine molecule has bidentate enediol ligands which can convert the coordinatively unsaturated iron surface sites back into a bulk-like lattice structure with an octahedral geometry for the oxygen-coordinated iron centers, resulting in tight binding of dopamine to iron oxide.[200] The resulting nanostructure can act as an anchor to further immobilize nitrilotriacetic acid molecules. This new material exhibits high specificity for protein separation and exceptional stability to heating and high salt concentrations.

Magnetic nanoparticles are ideal molecular carriers for gene separation owing to their high separation efficiency.[16,201] The collection and then the separation of rare DNA/mRNA targets which have single-base mismatches in a complex matrix is critically important in human disease diagnostics, gene expression studies, and gene profiling. Tan et al. have synthesized a genomagnetic nanocapturer (GMNC) for the collection, separation, and detection of trace amounts of DNA/RNA molecules with one single-base difference.[202] GMNC was fabricated with a magnetic nanoparticle as core, silica coating as a protecting and biocompatible layer, and avidin-biotin molecules as linkers for bioconjugating a molecular beacon as the DNA probe. It was demonstrated that GMNC shows highly efficient collection of trace amounts of DNA/mRNA samples down to femtomolar concentrations and is able to real-time monitor and confirm the collected gene products.

A very promising application of magnetic nanoparticles is in drug delivery as drug carriers, that is, so called "magnetic drug delivery" proposed in the 1970s by Widder et al.[203] The concept of magnetic targeting is to inject magnetic nanoparticles to which drug molecules are attached, to guide these particles to a chosen site under the localized magnetic field gradients, hold them there until the therapy is complete, and then to remove them. The magnetic drug carriers have the potential to carry a large dose of drug to achieve high local concentration, and avoid toxicity and other adverse side effects arising from high drug doses in other parts of the organism. Although considerable achievements have been reached in in vivo applications, to date, actual clinical studies are still problematic. Many fundamental issues in magnetic

drug delivery systems need to be solved, such as the size controlled synthesis and stability of magnetic nanoparticles, biocompatibility of the coating layers (polymer or silica), drug-particle binding, and the physiological parameters.[4,13]

Another interesting application of magnetic nanoparticles is in hyperthermia treatment which is considered as a supplementary treatment to chemotherapy, radiotherapy, and surgery in cancer therapy.[4,204,205] The idea of using magnetic induction hyperthermia is based on the fact that when magnetic nanoparticles are exposed to a varying magnetic field, heat is generated by the magnetic hysteresis loss, Néel-relaxation, and Brown-relaxation.[5,206] In an alternating magnetic field, induced currents are generate in metallic objects, and as a consequence, heat is generated in the metal. This phenomenon is greatly enhanced in metals showing collective magnetic behavior. Thus, when a magnetic fluid is exposed to an alternating magnetic field the particles become powerful heat sources, destroying tumor cells since these cells are more sensitive to temperatures in excess of 41 °C than their normal counterparts.

The heating of oxide magnetic materials with low electrical conductivity is mainly due to loss processes during the reorientation of the magnetization (so-called Néel-relaxation) or frictional forces if the particle can rotate in a medium of low viscosity (Brown-relaxation). The losses from the reorientation of magnetization (wall displacement for large particles or several types of rotational processes of magnetization for single-domain particles) are mainly determined by the intrinsic magnetic properties, such as magnetic anisotropy. As discussed in Section 2, for single-domain particles, the thermal fluctuations lead to an activation of the remagnetization process since the barrier energy decreases with decreasing particle size. An external magnetic field supplies energy and assists magnetic moments in overcoming the energy barrier. Besides the losses caused by magnetization rotation inside the particles, another loss type may arise in the case of ferrofluids which is related to the rotational Brownian motion of the magnetic particles. In this case, the energy barrier is determined by rotational friction within the suspension fluid of a certain viscosity.

The amount of heat generated by magnetic nanoparticles depends strongly on the structural properties of the particles (e.g., size, shape) and should be as high as possible to reduce the dose to a minimum level.

6. Summary and Perspectives

The synthesis of magnetic nanoparticles, covering a wide range of compositions and tunable sizes, has made substantial progress, especially over the past decade. However, synthesis of high-quality magnetic nanoparticles in a controlled manner, and detailed understanding of the synthetic mechanisms are still challenges to be faced in the coming years. Syntheses of oxide or metallic magnetic nanoparticles often require the use of toxic and/or expensive precursors, and the reaction is often performed in an organic phase at high temperature at high dilution. The nanoparticles obtained are usually dispersible only in organic solvents, not in an aqueous phase. Thus, the search for simple synthetic pathways for water-soluble metal oxides or even metallic nanoparticles with controlled size and shape will remain an active research field.

As a result of the dipolar interaction between the magnetic particles they are intriguing building blocks for self- or field-induced assembly into various nanostructures.[207] The assembly structures (1D, 2D, and 3D) are important for fundamental studies, and for the fabrication of magnetic-force triggered nanodevices. Recently, reports concerning the self-assembly of magnetic nanoparticles into specific shapes appeared. The synthesis of discrete 1D nanostructured magnetic materials, such as cobalt and iron nanorods, through the oriented attachment of monodisperse spherical nanoparticles has been described.[49,208,209] Self-assembly of cobalt nanoparticles with a size of approximately 9.2 nm and polydispersity of only 9% into 2D ordered structures has been performed by a vertical drying technique.[210] Cobalt nanocrystals (5–8 nm) can self-assemble into whisker shapes, if the carbonyl precursor is decomposed in an applied magnetic field.[210] More recently, Wang and co-workers reported a large-scale, hierarchical self-assembly of dendritic nanostructures of magnetic α-Fe_2O_3 (so-called micro-pine structure, as shown in Figure 12) through the hydrothermal

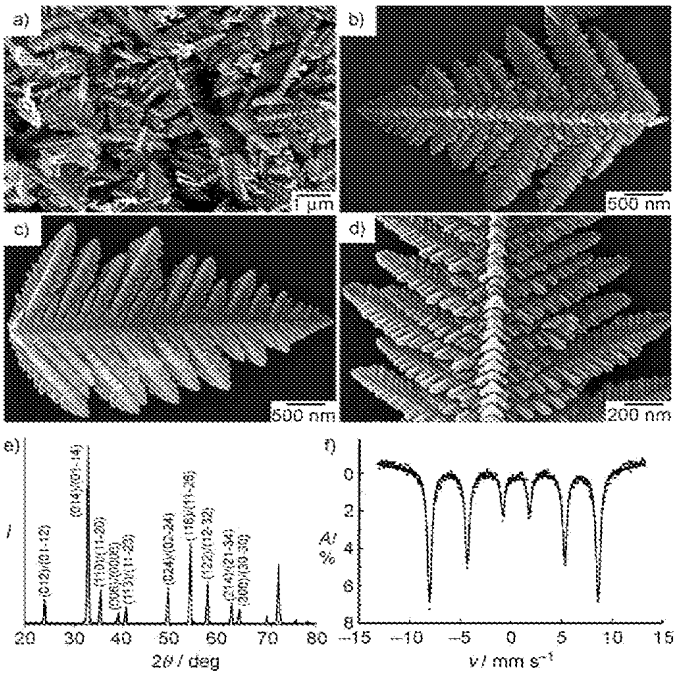

Figure 12. Electron microscopy images and chemical characterization of α-Fe_2O_3 fractals synthesized with a $K_3[Fe(CN)_6]$ concentration of 0.015 M at 140 °C. a) Low-magnification SEM image of fractals demonstrating good uniformity. b) SEM image of a single α-Fe_2O_3 fractal taken from one side. c) SEM image of a single α-Fe_2O_3 fractal taken from the other side. d) A higher magnification image of a single α-Fe_2O_3 fractal showing striking periodic corrugated structures on the main trunk. e) X-ray diffraction pattern of the sample confirming the formation of a pure α-Fe_2O_3 phase. f) Mössbauer spectrum of the sample recorded at room temperature showing the magnetic hyperfine splitting. Reproduced with kind permission from ref. [211].

reaction of $K_3[Fe(CN)_6]$ in aqueous solution at suitable temperatures.[211] The structure was formed as a result of fast growth along six crystallographically equivalent directions, and shows a lower Morin transition temperature of −57 °C. O'Brien and co-workers reported that PbSe semiconductor quantum dots and γ-Fe_2O_3 magnetic nanocrystals can arrange into precisely ordered 3D superlattices by self-assembly, wherein the size ratios determined the assembly of the magnetic and semiconducting nanoparticles into AB_{13} or AB_2 superlattices (Figure 13).[212] They suggested that this synthesis concept could ultimately enable the fine-tuning of material responses to magnetic, electrical, optical, and mechanical stimuli.

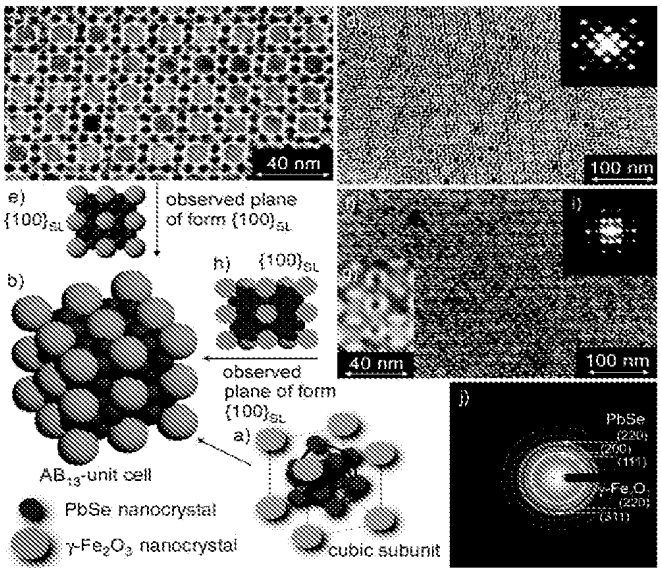

Figure 13. TEM micrographs and schematic representations of AB_{13} superlattices (isostructural with intermetallic phase $NaZn_{13}$, SG 226) of 11-nm γ-Fe_2O_3 and 6-nm PbSe nanocrystals. a) Cubic subunit of the AB_{13} unit cell. b) AB_{13} unit cell built up of eight cubic subunits. c) Projection of a $\{100\}_{SL}$ plane at high magnification SL = superlattice. d) As (c) but at low magnification; inset: small-angle electron diffraction pattern from a corresponding 6-μm^2 area. e) Depiction of a {100} plane. f) Projection of a $\{110\}_{SL}$ plane. g) As (f) but at high magnification. h) Depiction of the projection of the {110} plane. i) Small-angle electron diffraction pattern from a 6-μm^2 $\{110\}_{SL}$ area. j) Wide-angle electron diffraction pattern of an AB_{13}-superlattice (selected area electron diffraction (SAED) of a 6-μm^2 area) with indexing of the main diffraction rings for PbSe and γ-Fe_2O_3 (maghemite). Reproduced with kind permission from ref. [212].

Metallic nanoparticles have a higher magnetization than their oxidic counterparts. However, their high reactivity and toxicity make them unsuitable for direct applications in biomedicine/biotechnology. Therefore, metallic nanoparticles usually have to be protected with an isolating shell against the surrounding environment. For this purpose, coating with a polymer or a silica layer is often used. However, polymer-coated magnetic nanoparticles are not stable at high temperature, since the intrinsic instability of the polymers is further adversely affected by the catalytic properties of the nanoparticles. In the case of silica-coated magnetic nanoparticles, it is difficult or impossible to achieve a fully dense and nonporous silica coating, and it is thus difficult to maintain high stability of these nanoparticles under harsh conditions, especially in basic environments. There is still a need to explore novel synthetic methods to ensure the stability of magnetic nanoparticles at high temperatures and under acidic and basic conditions. Carbon-coated magnetic nanoparticles are remarkably stable under harsh conditions, but maintaining carbon-coated particles in an isolated, dispersible state proves to be very difficult.

Carbon-coated magnetic nanoparticles are conventionally prepared by arc-discharge, or laser ablation, where extremely high temperatures are required. These processes are often connected with a very poor yield and sometimes incomplete coating of the nanoparticles produced. The metallic nanoparticles thus obtained usually have a broad size distribution and are agglomerated to give big clusters, resulting in poor redispersibility. Thus, they are not suitable for uses in biotechnology and catalysis where small particles with a size of 10–200 nm are required.[213,214] The generation of a carbon coating on individual dispersed nanoparticles and the control of the shell thickness still remain unresolved problems.

Magnetic separation technology is a quick and easy means for separation and recycle of catalysts and other functional solids. We believe that the surface functionalization and modification of magnetic nanoparticles to introduce additional functionality will gain more and more attention. Complex, multifunctional magnetic nanoparticle systems with designed active sites, including ligands, enzymes, chiral catalysts, drugs, and other species, seem to be promising for a variety of applications. Whether industrial applications of such systems can be achieved and how far we can go in all those areas will depend on our ability to synthesize stable and robust magnetic nanoparticles which can withstand the conditions encountered in these applications in an economical and scalable fashion.

Received: July 18, 2006

[1] S. Chikazumi, S. Taketomi, M. Ukita, M. Mizukami, H. Miyajima, M. Setogawa, Y. Kurihara, *J. Magn. Magn. Mater.* **1987**, *65*, 245.
[2] A.-H. Lu, W. Schmidt, N. Matoussevitch, H. Bönnermann, B. Spliethoff, B. Tesche, E. Bill, W. Kiefer, F. Schüth, *Angew. Chem.* **2004**, *116*, 4403; *Angew. Chem. Int. Ed.* **2004**, *43*, 4303.
[3] S. C. Tsang, V. Caps, I. Paraskevas, D. Chadwick, D. Thompsett, *Angew. Chem.* **2004**, *116*, 5763; *Angew. Chem. Int. Ed.* **2004**, *43*, 5645.
[4] A. K. Gupta, M. Gupta, *Biomaterials* **2005**, *26*, 3995.
[5] S. Mornet, S. Vasseur, F. Grasset, P. Verveka, G. Goglio, A. Demourgues, J. Portier, E. Pollert, E. Duguet, *Prog. Solid State Chem.* **2006**, *34*, 237.
[6] Z. Li, L. Wei, M. Y. Gao, H. Lei, *Adv. Mater.* **2005**, *17*, 1001.
[7] T. Hyeon, *Chem. Commun.* **2003**, 927.
[8] D. W. Elliott, W.-X. Zhang, *Environ. Sci. Technol.* **2001**, *35*, 4922.
[9] M. Takafuji, S. Ide, H. Ihara, Z. Xu, *Chem. Mater.* **2004**, *16*, 1977.
[10] D. C. Jiles, *Acta Mater.* **2003**, *51*, 5907.

[11] O. V. Salata, *J. Nanobiotechnol.* **2004**, *2*, 3.
[12] G. Barratt, *Cell. Mol. Life Sci.* **2003**, *60*, 21.
[13] T. Neuberger, B. Schöpf, H. Hofmann, M. Hofmann, B. von Rechenberg, *J. Magn. Magn. Mater.* **2005**, *293*, 483.
[14] C. C. Berry, *J. Mater. Chem.* **2005**, *15*, 543.
[15] P. Tartaj, M. del Puerto Morales, S. Veintemillas-Verdaguer, T. Gonzalez-Carreno, C. J. Serna, *J. Phys. D* **2003**, *36*, R182.
[16] H. Gu, K. Xu, C. Xu, B. Xu, *Chem. Commun.* **2006**, 941.
[17] V. S. Kalambur, B. Han, B. E. Hammer, T. W. Shield, J. C. Bischof, *Nanotechnology* **2005**, *16*, 1221.
[18] D. L. Huber, *Small* **2005**, *1*, 482.
[19] X. Batlle, A. Labarta, *J. Phys. D* **2002**, *35*, R15.
[20] C. M. Sorensen, *Magnetism in Nanoscale Materials in Chemistry* (Ed.: K. J. Klabunde), Wiley-Interscience Publication, New York, **2001**.
[21] T. Iwaki, Y. Kakihara, T. Toda, M. Abdullah, K. Okuyama, *J. Appl. Phys.* **2003**, *94*, 6807.
[22] A. Ney, P. Poulopoulos, M. Farle, K. Baberschke, *Phys. Rev. B* **2000**, 62, 11336, and references therein.
[23] S. Foner, *Rev. Sci. Instrum.* **1959**, *30*, 548.
[24] M. Farle, *Rep. Prog. Phys.* **1998**, *61*, 755.
[25] H. Elbert, *Rep. Prog. Phys.* **1996**, *59*, 1665.
[26] J. Stöhr, *J. Magn. Magn. Mater.* **1999**, 200, 470.
[27] B. Hillebrands, G. Güntherodt *Ultrathin Magnetic Structure, Vols I and II*, Berlin, Springer, **1994**.
[28] R. H. Kodama, *J. Magn. Magn. Mater.* **1999**, *200*, 359.
[29] M. Respaud, J. M. Broto, H. Rakoto, A. R. Fert, L. Thomas, B. Barbara, M. Verelst, E. Snoeck, P. Lecante, A. Mosset, J. Osuna, T. Ould Ely, C. Amiens, B. Chaudret, *Phys. Rev. B* **1998**, *57*, 2925.
[30] F. Bødker, S Mørup, S. Linderoth, *Phys. Rev. Lett.* **1994**, *72*, 282.
[31] W. S. Seo, H. H. Jo, K. Lee, B. Kim, S. J. Oh, J. T. Park, *Angew. Chem.* **2004**, *116*, 1135; *Angew. Chem. Int. Ed.* **2004**, *43*, 1115.
[32] T. Hyeon, S. S. Lee, J. Park, Y. Chung, H. B. Na, *J. Am. Chem. Soc.* **2001**, *123*, 12798.
[33] S. I. Makhlouf, *J. Magn. Magn. Mater.* **2002**, *246*, 184.
[34] Y. Wang, C.-M. Yang, W. Schmidt, B. Spliethoff, E. Bill, F. Schüth, *Adv. Mater.* **2005**, *17*, 53.
[35] A. Homola, M. Lorenz, C. Mastrangelo, T. Tilbury, *IEEE Trans. Magn.* **2003**, *22*, 716.
[36] P. M. Paulus, H. Bönnemann, A. M. van der Kraan, F. Luis, J. Sinzig, L. J. de Jongh, *Eur. Phys. J. D* **1999**, *9*, 501.
[37] J. Hormes, H, Modrow, H. Bönnemann, C. S. S. R. Kumar, *J. Appl. Phys.* **2005**, *97*, 10R102.
[38] D. A. van Leeuwen, J. M. van Ruitenbeek, L. J. de Jongh, A. Ceriotti, G. Pacchioni, O. D. Häberlen, N. Rösch, *Phys. Rev. Lett.* **1994**, *73*, 1432.
[39] N. Cordente, M. Respaud, F. Senocq, M-J. Casanove, C. Amiens, B. Chaudret, *Nano Lett.* **2001**, *1*, 565.
[40] J. Nogués, J. Sort, V. Langlais, V. Skumryev, S. Suriñach, J. S. Muñoz, M. D. Baró, *Phys. Rep.* **2005**, *422*, 65.
[41] E. L. Salabas, A. Rumplecker, F. Kleitz, F. Radu, F. Schüth, *Nano Lett.* **2006**, *6*, 2977.
[42] V. Skumryev, S. Stoyanov, Y. Zhang, G. Hadjipanayis, D. Givord, J. Nogues, *Nature* **2003**, *423*, 850.
[43] H. Zeng, J. Li, L. Zhong, S. Sun, *Nature* **2002**, *420*, 395.
[44] H. Zeng, S. Sun, J. Li, Z. L. Wang, J. P. Liu, *Appl. Phys. Lett.* **2004**, *85*, 792.
[45] S. Neveu, A. Bee, M. Robineau, D. Talbot, *J. Colloid Interface Sci.* **2002**, *255*, 293.
[46] F. Grasset, N. Labhsetwar, D. Li, D. C. Park, N. Saito, H. Haneda, O. Cador, T. Roisnel, S. Mornet, E. Duguet, J. Portier, J. Etourneau, *Langmuir* **2002**, *18*, 8209.
[47] S. Sun, H. Zeng, *J. Am. Chem. Soc.* **2002**, *124*, 8204.
[48] S.-J. Park, S. Kim, S. Lee, Z. Khim, K. Char, T. Hyeon, *J. Am. Chem. Soc.* **2000**, *122*, 8581.
[49] V. F. Puntes, K. M. Krishan, A. P. Alivisatos, *Science* **2001**, *291*, 2115.
[50] Q. Chen, A. J. Rondinone, B. C. Chakoumakos, Z. J. Zhang, *J. Magn. Magn. Mater.* **1999**, *194*, 1.
[51] J. Park, K. An, Y. Hwang, J.-G. Park, H.-J. Noh, J.-Y. Kim, J.-H. Park, N.-M. Hwang, T. Hyeon, *Nat. Mater.* **2004**, *3*, 891.
[52] S. Sun, C. B. Murray, D. Weller, L. Folks, A. Moser, *Science* **2000**, *287*, 1989.
[53] E. V. Shevchenko, D. V. Talapin, A. L. Rogach, A. Kornowski, M. Haase, H. Weller, *J. Am. Chem. Soc.* **2002**, *124*, 11480.
[54] J. Lee, T. Isobe, M. Senna, *Colloids Surf. A* **1996**, *109*, 121.
[55] A. Bee, R. Massart, S. Neveu, *J. Magn. Magn. Mater.* **1995**, *149*, 6.
[56] T. Ishikawa, S. Kataoka, K. Kandori, *J. Mater. Sci.* **1993**, *28*, 2693.
[57] T. Ishikawa, T. Takeda, K. Kandori, *J. Mater. Sci.* **1992**, *27*, 4531.
[58] K. Kandori, Y. Kawashima, T. Ishikawa, *J. Colloid Interface Sci.* **1992**, *152*, 284.
[59] R. M. Cornell, P. W. Schindler, *Colloid Polym. Sci.* **1980**, *258*, 1171.
[60] A. L. Willis, N. J. Turro, S. O'Brien, *Chem. Mater.* **2005**, *17*, 5970.
[61] B. L. Cushing, V. L. Kolesnichenko, C. J. O'Connor, *Chem. Rev.* **2004**, *104*, 3893.
[62] C. B. Murray, D. J. Norris, M. G. Bawendi, *J. Am. Chem. Soc.* **1993**, *115*, 8706.
[63] X. Peng, J. Wickham, A. P. Alivisatos, *J. Am. Chem. Soc.* **1998**, *120*, 5343.
[64] S. O'Brien, L. Brus, C. B. Murray, *J. Am. Chem. Soc.* **2001**, *123*, 12085.
[65] S. Sun, H. Zeng, D. B. Robinson, S. Raoux, P. M. Rice, S. X. Wang, G. Li, *J. Am. Chem. Soc.* **2004**, *126*, 273.
[66] F. X. Redl, C. T. Black, G. C. Papaefthymiou, R. L. Sandstrom, M. Yin, H. Zeng, C. B. Murray, S. P. O'Brien, *J. Am. Chem. Soc.* **2004**, *126*, 14583.
[67] J. Rockenberger, E. C. Scher, A. P. Alivisatos, *J. Am. Chem. Soc.* **1999**, *121*, 11595.
[68] D. Farrell, S. A. Majetich, J. P. Wilcoxon, *J. Phys. Chem. B* **2003**, *107*, 11022.
[69] N. R. Jana, Y. Chen, X. Peng, *Chem. Mater.* **2004**, *16*, 3931.
[70] A. C. S. Samia, K. Hyzer, J. A. Schlueter, C.-J. Qin, J. S. Jiang, S. D. Bader, X.-M. Lin, *J. Am. Chem. Soc.* **2005**, *127*, 4126.
[71] Y. Li, M. Afzaal, P. O'Brien, *J. Mater. Chem.* **2006**, *16*, 2175.
[72] T. Hyeon, S. S. Lee, J. Park, Y. Chung, H. B. Na, *J. Am. Chem. Soc.* **2001**, *123*, 12798.
[73] S. Sun, H. Zeng, D. B. Robinson, S. Raoux, P. M. Rice, S. X. Wang, G. Li, *J. Am. Chem. Soc.* **2004**, *126*, 273.
[74] J. Park, E. Lee, N.-M. Hwang, M. Kang, S. C. Kim, Y. Hwang, J.-G. Park, H.-J. Noh, J.-Y. Kim, J.-H. Park, T. Hyeon, *Angew. Chem.* **2005**, *117*, 2931; *Angew. Chem. Int. Ed.* **2005**, *44*, 2872.
[75] V. K. LaMer, R. H. Dinegar, *J. Am. Chem. Soc.* **1950**, *72*, 4847.
[76] Z. Li, Q. Sun, M. Gao, *Angew. Chem.* **2005**, *117*, 125; *Angew. Chem. Int. Ed.* **2005**, *44*, 123.
[77] F. Q. Hu, L. Wei, Z. Zhou, Y. L. Ran, Z. Li, M. Y. Gao, *Adv. Mater.*, **2006**, *18*, 2553.
[78] K. Butter, A. P. Philipse, G. J. Vroege, *J. Magn. Magn. Mater.* **2002**, *252*, 1.
[79] F. Dumestre, B. Chaudret, C. Amiens, P. Renaud, P. Fejes, *Science* **2004**, *303*, 821.
[80] Q. Song, Z. J. Zhang, *J. Am. Chem. Soc.* **2004**, *126*, 6164.
[81] V. F. Puntes, D. Zanchet, C. K. Erdonmez, A. P. Alivisatos, *J. Am. Chem. Soc.* **2002**, *124*, 12874.
[82] F. Dumestre, B. Chaudret, C. Amiens, M.-C. Fromen, M.-J. Casanove, M. Respaud, P. Zurcher, *Angew. Chem.* **2002**, *114*, 4462; *Angew. Chem. Int. Ed.* **2002**, *41*, 4286.

[83] F. Dumestre, B. Chaudret, C. Amiens, M. Respaud, P. Fejes, P. Renaud, P. Zurcher, *Angew. Chem.* **2003**, *115*, 5371; *Angew. Chem. Int. Ed.* **2003**, *42*, 5213.
[84] H. Bönnemann, W. Brijoux, R. Brinkmann, N. Matoussevitch, N. Waldoefner, N. Palina, H. Modrow, *Inorg. Chim. Acta.* **2003**, *350*, 617.
[85] Y. Yamada, T. Suzuki, E. N. Abarra, *IEEE Trans. Magn.* **1998**, *34*, 343.
[86] C. M. Lukehart, S. B. Milne, S. R. Stock, *Chem. Mater.* **1998**, *10*, 903.
[87] C. Stinner, R. Prins, T. Weber, *J. Catal.* **2001**, *202*, 187.
[88] O. Tegus, E. Brück, K. H. J. Buschow, F. R. de Boer, *Nature* **2002**, *415*, 150.
[89] F. Luo, H.-L Su, W. Song, Z.-M. Wang, Z.-G. Yan, C.-H. Yan, *J. Mater. Chem.* **2004**, *14*, 111.
[90] K. L. Stamm, J. C. Garno, G.-y. Liu, S. L. Brock, *J. Am. Chem. Soc.* **2003**, *125*, 4038.
[91] S. C. Perera, G. Tsoi, L. E. Wenger, S. L. Brock, *J. Am. Chem. Soc.* **2003**, *125*, 13960.
[92] C. Qian, F. Kim, L. Ma, F. Tsui, P. Yang, J. Liu, *J. Am. Chem. Soc.* **2004**, *126*, 1195.
[93] J. Park, B. Koo, Y. Hwang, C. Bae, K. An, J.-G. Park, H. M. Park, T. Hyeon, *Angew. Chem.* **2004**, *116*, 2332; *Angew. Chem. Int. Ed.* **2004**, *43*, 2282.
[94] D. Langevin, *Annu. Rev. Phys. Chem.* **1992**, *43*, 341.
[95] B. K. Paul, S. P. Moulik, *Curr. Sci.* **2001**, *80*, 990.
[96] E. E. Carpenter, C. T. Seip, C. J. O'Connor, *J. Appl. Phys.* **1999**, *85*, 5184.
[97] C. Liu, B. Zou, A. J. Rondinone, Z. J. Zhang, *J. Phys. Chem. B* **2000**, *104*, 1141.
[98] K. Woo, H. J. Lee, J.-P. Ahn, Y. S. Park, *Adv. Mater.* **2003**, *15*, 1761.
[99] N. Moumen, M. P. Pileni, *J. Phys. Chem.* **1996**, *100*, 1867.
[100] W. Tan, S. Santra, P. Zhang, R. Tapec, J. Dobson, US Patent 6548264, **2003**.
[101] X. Wang, J. Zhuang, Q. Peng, Y Li, *Nature* **2005**, *437*, 121.
[102] H. Deng, X. Li, Q. Peng, X. Wang, J. Chen, Y. Li, *Angew. Chem.* **2005**, *117*, 2841; *Angew. Chem. Int. Ed.* **2005**, *44*, 2782.
[103] L. E. Euliss, S. G. Grancharov, S. O'Brien, T. J. Deming, G. D. Stucky, C. B. Murray, G. A. Held, *Nano Lett.* **2003**, *3*, 1489.
[104] X. Liu, Y. Guan, Z. Ma, H. Liu, *Langmuir* **2004**, *20*, 10278.
[105] R. Hong, N. O. Fischer, T. Emrick, V. M. Rotello, *Chem. Mater.* **2005**, *17*, 4617.
[106] Y. Sahoo, H. Pizem, T. Fried, D. Golodnitsky, L. Burstein, C. N. Sukenik, G. Markovich, *Langmuir* **2001**, *17*, 7907.
[107] M. Kim, Y. Chen, Y. Liu, X. Peng, *Adv. Mater.* **2005**, *17*, 1429.
[108] Y. Kobayashi, M. Horie, M. Konno, B. Rodriguez-Gonzalez, L. M. Liz-Marzan, *J. Phys. Chem. B* **2003**, *107*, 7420.
[109] A.-H. Lu, W. Li, N. Matoussevitch, B. Spliethoff, H. Bönnemann, F. Schüth, *Chem. Commun.* **2005**, 98.
[110] N. S. Sobal, M. Hilgendorff, H. Moehwald, M. Giersig, M. Spasova, T. Radetic, M. Farle, *Nano Lett.* **2002**, *2*, 62.
[111] Q. Liu, Z. Xu, J. A. Finch, R. Egerton, *Chem. Mater.* **1998**, *10*, 3936.
[112] J. Lin, W. Zhou, A. Kumbhar, J. Wiemann, J. Fang, E. E. Carpenter, C. J. O'Connor, *J. Solid State Chem.* **2001**, *159*, 26.
[113] N. O. Nunez, P. Tartaj, M. P. Morales, P. Bonville, C. J. Serna, *Chem. Mater.* **2004**, *16*, 3119.
[114] D. K. Kim, M. Mikhaylova, Y. Zhang, M. Muhammed, *Chem. Mater.* **2003**, *15*, 1617.
[115] D. L. Peng, K. Sumiyama, T. Hihara, S. Yamamuro, T. J. Konno, *Phys. Rev. B* **2000**, *61*, 3103.
[116] H.-G. Boyen, G. Kästle, K. Zürn, T. Herzog, F. Weigl, P. Ziemann, O. Mayer, C. Jerome, M. Möller, J. P. Spatz, M. G. Garnier, P. Oelhafen, *Adv. Funct. Mater.* **2003**, *13*, 359.
[117] S. S. Papell, US Patent 3215572, **1965**.
[118] R. Massart, *IEEE Trans. Magn.* **1981**, *MAG-17*, 1247.
[119] K. Raj, R. Moskowitz, *J. Magn. Magn. Mater.* **1990**, *85*, 107.
[120] M. De Cuyper, M. Joniau, *Langmuir* **1991**, *7*, 647.
[121] A. Wooding, M. Kilner, D. Lambrick, *J. Colloid Interface Sci.* **1992**, *149*, 98.
[122] D. Zins, V. Cabuil, R. Massart, *J. Mol. Liq.* **1999**, *83*, 217.
[123] L. Shen, P. E. Laibinis, T. A. Hatton, *Langmuir* **1999**, *15*, 447.
[124] M. H. Sousa, F. A. Tourinho, J. Depeyrot, G. J. da Silva, M. C. F. L. Lara, *J. Phys. Chem. B* **2001**, *105*, 1168.
[125] R. M. Cornell, U. Schertmann, *The Iron Oxides: Structure, Properties, Reactions, Occurrence and Uses*, VCH, Weinheim, **1996**.
[126] M. Wan, J. Li, *J. Polymer. Sci.* **1998**, *36*, 2799.
[127] M. D. Butterworth, S. A. Bell, S. P. Armes, A. W. Simpson, *J. Colloid Interface Sci.* **1996**, *183*, 91.
[128] P. Tartaj, M. P. Morales, T. González-Carreno, S. Veintemillas-Verdaguer, C. J. Serna, *J. Magn. Magn. Mater.* **2005**, *28*, 290.
[129] G. Barratt, *Cell. Mol. Life Sci.* **2003**, *60*, 21.
[130] L. A. Harris, J. D. Goff, A. Y. Carmichael, J. S. Riffle, J. J. Harburn, T. G. St. Pierre, M. Saunders, *Chem. Mater.* **2003**, *15*, 1367.
[131] A. F. Thunemann, D. Schutt, L. Kaufner, U. Pison, H. Möhwald, *Langmuir* **2006**, *22*, 2351.
[132] P. A. Dresco, V. S. Zaitsev, R. J. Gambino, B. Chu, *Langmuir* **1999**, *15*, 1945.
[133] J. Deng, X. Ding, W. Zhang, Y. Peng, J. Wang, X. Long, P. Li, A. S. C. Chan, *Polymer* **2002**, *43*, 2179.
[134] X. Xu, G. Friedman, K. Humfeld, S. Majetich, S. Asher, *Adv. Mater.* **2001**, *13*, 1681.
[135] C. R. Vestal, Z. J. Zhang, *J. Am. Chem. Soc.* **2002**, *124*, 14312.
[136] Y. Wang, X. Teng, J.-S. Wang, H. Yang, *Nano Lett.* **2003**, *3*, 789.
[137] J. Rivas, R. D. Sánchez, A. Fondado, C. Izco, A. J. García-Bastida, J. García-Otero, J. Mira, D. Baldomir, A. González, I. Lado, M. A. López-Quintela, S. B. Oseroff, *J. Appl. Phys.* **1994**, *76*, 6564.
[138] E. E. Carpenter, C. Sangregorio, C. J. O'Connor, *IEEE Trans. Magn.* **1999**, *35*, 3496.
[139] J.-I. Park, J. Cheon, *J. Am. Chem. Soc.* **2001**, *123*, 5743.
[140] Z. Ban, Y. A. Barnakov, F. Li, V. O. Golub, C. J. O'Connor, *J. Mater. Chem.* **2005**, *15*, 4660.
[141] Y. Shon, G. B. Dawson, M. Porter, R. W. Murray, *Langmuir* **2002**, *18*, 3880.
[142] J. L. Lyon, D. A. Fleming, M. B. Stone, P. Schiffer, M. E. Williams, *Nano Lett.* **2004**, *4*, 719.
[143] S.-J. Cho, J.-C. Idrobo, J. Olamit, K. Liu, N. D. Browning, S. M. Kauzlarich, *Chem. Mater.* **2005**, *17*, 3181.
[144] H. Yu, M. Chen, P. M. Rice, S. X. Wang, R. L. White, S. Sun, *Nano Lett.* **2005**, *5*, 379.
[145] L. Wang, J. Luo, M. M. Maye, Q. Fan, Q. Rendeng, M. H. Engelhard, C. Wang, Y. Lin, C.-J. Zhong, *J. Mater. Chem.* **2005**, *15*, 1821.
[146] D. Caruntu, B. L. Cushing, G. Caruntu, C. J. O'Connor, *Chem. Mater.* **2005**, *17*, 3398.
[147] J. Zhang, M. Post, T. Veres, Z. J. Jakubek, J. Guan, D. Wang, F. Normandin, Y. Deslandes, B. Simard, *J. Phys. Chem. B* **2006**, *110*, 7122.
[148] Z. Guo, C. S. S. R. Kumar, L. L. Henry, C. K. Saw, J. Hormes, E. J. Podlaha, 49th Magnetism and Magnetic Materials (MMM) Annual Conference Proceedings, **2004**, S. 366.
[149] Z. Lu, M. D. Prouty, Z. Guo, V. O. Golub, C. S. S. R. Kumar, Y. M. Lvov, *Langmuir* **2005**, *21*, 2042.
[150] V. L. Colvin, A. N. Goldstein, A. P. Alivisatos, *J. Am. Chem. Soc.* **1992**, *114*, 5221.
[151] D. Ma, J. Guan, F. Normandin, S. Denommee, G. Enright, T. Veres, B. Simard, *Chem. Mater.* **2006**, *18*, 1920.
[152] W. Stöber, A. Fink, E. J. Bohn, *J. Colloid Interface Sci.* **1968**, *26*, 62.

[153] T. Tago, T. Hatsuta, K. Miyajima, M. Kishida, S. Tashiro, K. Wakabayashi, *J. Am. Ceram. Soc.* **2002**, *85*, 2188.
[154] Y. Lu, Y. Yin, B. T. Mayers, Y. Xia, *Nano Lett.* **2002**, *2*, 183.
[155] C. Graf, D. L. J. Vossen, A. Imhof, A. Van Blaaderen, *Langmuir* **2003**, *19*, 6693.
[156] A. P. Philipse, M. P. B. van Bruggen, C. Pathmamanoharan, *Langmuir* **1994**, *10*, 92.
[157] A. Ulman, *Chem. Rev.* **1996**, *96*, 1533.
[158] M. Ohmori, E. Matijevic, *J. Colloid Interface Sci.* **1992**, *150*, 594.
[159] M. A. Correa-Duarte, M. Giersig, N. A. Kotov, L. M. Liz-Marzán, *Langmuir* **1998**, *14*, 6430.
[160] M. Ohmori, E. Matijevic, *J. Colloid Interface Sci.* **1993**, *160*, 288.
[161] Y. Kobayashi, M. Horie, M. Konno, B. Rodriguez-González, L. M. Liz-Marzan, *J. Phys. Chem. B* **2003**, *107*, 7420.
[162] W. Zhao, J. Gu, L. Zhang, H. Chen, J. Shi, *J. Am. Chem. Soc.* **2005**, *127*, 8916.
[163] S. Santra, R. Tapec, N. Theodoropoulou, J. Dobson, A. Hebrad, W. Tan, *Langmuir* **2001**, *17*, 2900.
[164] D. K. Yi, S. S. Lee, G. C. Papaefthymiou, J. Y. Ying, *Chem. Mater.* **2006**, *18*, 614.
[165] P. Tartaj, C. J. Serna, *J. Am. Chem. Soc.* **2003**, *125*, 15754.
[166] C. R. Vestal, Z. J. Zhang, *Nano Lett.* **2003**, *3*, 1739.
[167] L. M. Liz-Marzán, M. Giersig, P. Mulvaney, *Chem. Commun.* **1996**, 731.
[168] T. Ung, L. M. Liz-Marzán, P. Mulvaney, *Langmuir* **1998**, *14*, 3740.
[169] J. H. J. Scott, S. A. Majetich, *Phys. Rev. B* **1995**, *52*, 12564.
[170] K. H. Ang, I. Alexandrou, N. D. Mathur, G. A. J. Amaratunga, S. Haq, *Nanotechnology* **2004**, *15*, 520.
[171] W. Teunissen, F. M. F. de Groot, J. Geus, O. Stephan, M. Tence, C. Colliex, *J. Catal.* **2001**, *204*, 169.
[172] T. Hayashi, S. Hirono, M. Tomita, S. Umemura, *Nature* **1996**, *381*, 772.
[173] R. Nesper, A. Ivantchenko, F. Krumeich, *Adv. Funct. Mater.* **2006**, *16*, 296.
[174] H. B. S. Chan, B. L. Ellis, H. L. Sharma, W. Frost, V. Caps, R. A. Shields, S. C. Tsang, *Adv. Mater.* **2004**, *16*, 144.
[175] S. I. Nikitenko, Y. Koltypin, O. Palchik, I. Felner, X. N. Xu, A. Gedanken, *Angew. Chem.* **2001**, *113*, 4579; *Angew. Chem. Int. Ed.* **2001**, *40*, 4447.
[176] J. Geng, D. A. Jefferson, B. F. G. Johnson, *Chem. Commun.* **2004**, 2442.
[177] V. V. Baranauskas, M. A. Zalich, M. Saunders, T. G. St. Pierre, J. S. Riffle, *Chem. Mater.* **2005**, *17*, 5246.
[178] A.-H. Lu, W. Li, E.-L. Salabas, B. Spliethoff, F. Schüth, *Chem. Mater.* **2006**, *18*, 2086.
[179] S. I. Stoeva, F. Huo, J.-S. Lee, C. A. Mirkin, *J. Am. Chem. Soc.* **2005**, *127*, 15362.
[180] D. K. Yi, S. T. Selvan, S. S. Lee, G. C. Papaefthymiou, D. Kundaliya, J. Y. Ying, *J. Am. Chem. Soc.* **2005**, *127*, 4990.
[181] F. Caruso, M. Spasova, A. Susha, M. Giersig, R. A. Caruso, *Chem. Mater.* **2001**, *13*, 109.
[182] P. Tartaj, T. González-Carreño, C. J. Serna, *Adv. Mater.* **2001**, *13*, 1620.
[183] M. A. Correa-Duarte, M. Grzelczak, V. Salgueirino-Maceira, M. Giersig, L. M. Liz-Marzan, M. Farle, K. Sierazdki, R. Diaz, *J. Phys. Chem. B* **2005**, *109*, 19060.
[184] A. Dyal, K. Loos, M. Noto, S. W. Chang, C. Spagnoli, K. V. P. M. Shafi, A. Ulman, M. Cowman, R. A. Gross, *J. Am. Chem. Soc.* **2003**, *125*, 1684.
[185] R. Hirsch, E. Katz, I. Willner, *J. Am. Chem. Soc.* **2000**, *122*, 12053.
[186] I. Willner, E. Katz, *Angew. Chem.* **2003**, *115*, 4724; *Angew. Chem. Int. Ed.* **2003**, *42*, 4576.
[187] V. Salgueiriño-Maceira, M. A. Correa-Duarte, M. Farle, A. López-Quintela, K. Sieradzki, R. Diaz, *Chem. Mater.* **2006**, *18*, 2701.
[188] Y. Deng, W. Yang, C. Wang, S. Fu, *Adv. Mater.* **2003**. *15*, 1729.
[189] B. L. Frankamp, N. O. Fischer, R. Hong, S. Srivastava, V. M. Rotello *Chem. Mater.* **2006**, *18*, 956.
[190] S. Giri, B. G. Trewyn, M. P. Stellmaker, V. S.-Y. Lin, *Angew. Chem.* **2005**, *117*, 5166; *Angew. Chem. Int. Ed.* **2005**, *44*, 5038.
[191] C. Bergemann, D. Muller-Schulte, J. Oster, L. Brassard, A. S. Lubbe, *J. Magn. Magn. Mater.* **1999**, *194*, 45.
[192] L. Nunez, M. D. Kaminski, *J. Magn. Magn. Mater.* **1999**, *194*, 102.
[193] A. Hu, G. T. Yee, W. Lin, *J. Am. Chem. Soc.* **2005**, *127*, 12486.
[194] C.-H. Jun, Y. J. Park, Y.-R. Yeon, J. Choi, W. Lee, S. Ko, J. Cheon, *Chem. Commun.* **2006**, 1619.
[195] R. B. Bedford, M. Betham, D. W. Bruce, S. A. Davis, R. M. Frost, M. Hird, *Chem. Commun.* **2006**, 1398.
[196] A.-H. Lu, W. Li, A. Kiefer, W. Schmidt, E. Bill, G. Fink, F. Schüth, *J. Am. Chem. Soc.* **2004**, *126*, 8616.
[197] J. Lee, D. Lee, E. Oh, J. Kim, Y.-P. Kim, S. Jin, H.-S. Kim, Y. Hwang, J. H. Kwak, J.-G. Park, C.-H. Shin, J. Kim, T. Hyeon, *Angew. Chem.* **2005**, *117*, 7593; *Angew. Chem. Int. Ed.* **2005**, *44*, 7427.
[198] J. Kim, J. E. Lee, J. Lee, J. H. Yu, B. C. Kim, K. An, Y. Hwang, C.-H. Shin, J.-G. Park, J. Kim, T. Hyeon, *J. Am. Chem. Soc.* **2006**, *128*, 688.
[199] C. Xu, K. Xu, H. Gu, R. Zheng, H. Liu, X. Zhang, Z. Guo, B. Xu, *J. Am. Chem. Soc.* **2004**, *126*, 9938.
[200] L. X. Chen, T. Li, M. C. Thurnauer, R. Csencsits, T. Rajh, *J. Phys. Chem. B* **2002**, *106*, 8539.
[201] I. Safarik, M. Safarikova, *J. Chromatogr. B* **1999**, *722*, 33.
[202] X. Zhao, R. Tapec-Dytioco, K. Wang, W. Tan, *Anal. Chem.* **2003**, *75*, 3476.
[203] K. J. Widder, A. E. Senyei, D. G. Scarpelli, *Proc. Soc. Exp. Biol. Med.* **1978**, *58*, 141.
[204] C. C Berry, A. S. G. Curtis, *J. Phys. D* **2003**, *36*, R198.
[205] S. Mornet, S. Vasseur, F. Grasset, E. Duguet, *J. Mater. Chem.* **2004**, *14*, 2116.
[206] R. Hiergeist, W. Andrä, N. Buske, R. Hergt, I. Hilger, U. Richter, W. Kaiser, *J. Magn. Magn. Mater.* **1999**, *201*, 420.
[207] M. Giersig, M. Hilgendorff, *Eur. J. Inorg. Chem.* **2005**, 3571.
[208] S.-J. Park, S. Kim, S. Lee, Z. G. Khim, K. Char, T. Hyeon, *J. Am. Chem. Soc.* **2000**, *122*, 8581.
[209] K. S. Suslick, M. Fang, T. Hyeon, *J. Am. Chem. Soc.* **1996**, *118*, 11960.
[210] J. S. Yin, Z. L. Wang, *Nanostruct. Mater.* **1999**, *11*, 845.
[211] M. Cao, T. Liu, S. Gao, G. Sun, X. Wu, C. Hu, Z. L. Wang, *Angew. Chem.* **2005**, *117*, 4269; *Angew. Chem. Int. Ed.* **2005**, *44*, 4197.
[212] F. X. Redl, K.-S. Cho, C. B. Murray, S. O'Brien, *Nature* **2003**, *423*, 968.
[213] X. Gao, K. M. K. Yu, K. Y. Tam, S. C. Tsang, *Chem. Commun.* **2003**, 2998.
[214] M. Wu, Y. D. Zhang, S. Hui, T. D. Xiao, S. Ge, W. A. Hines, J. I. Budnick, *J. Appl. Phys.* **2002**, *92*, 491.

